Climate Risk Management 40 (2023) 100511

Contents lists available at ScienceDirect

Climate Risk Management

journal homepage: www.elsevier.com/locate/crm

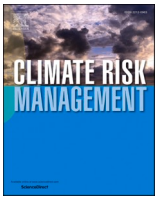

Quantifying uncertainty and sensitivity in climate risk assessments: Varying hazard, exposure and vulnerability modelling choices

Laura C. Dawkins [a], Dan J. Bernie [a,b], Francesca Pianosi [c,d], Jason A. Lowe [a,e], Theodoros Economou [f]

[a] Met Office, Fitzroy Road, Exeter, Devon EX1 3PB, United Kingdom
[b] Faculty of Health Sciences, University of Bristol, Bristol, UK
[c] Department of Civil Engineering, University of Bristol, United Kingdom
[d] Cabot Institute for the Environment, University of Bristol, United Kingdom
[e] Priestley International Centre for Climate, University of Leeds, Leeds, UK
[f] Climate and Atmosphere Research Center, The Cyprus Institute, Cyprus

ARTICLE INFO

Keywords:
Climate risk
Risk assessment
Uncertainty analysis
Sensitivity analysis

ABSTRACT

Open-source climate risk assessment platforms allow for accessible and efficient estimation of current and future climate risk by combining information about hazard, exposure and vulnerability. Such assessments require making a number of choices, such as which hazard data source to use, and the data and approach taken to represent the exposure and vulnerability. As these choices are, to some extent, subjective, when assessing risk and informing adaptation decisions, alternative options should be considered to understand the uncertainty and sensitivity of risk to uncertain input data and assumptions. We present a novel approach to quantify the uncertainty and sensitivity of risk estimates, using the CLIMADA open-source climate risk assessment platform. This work builds upon a recently developed extension of CLIMADA, which uses statistical modelling techniques to model and stochastically simulate alternative realisations of climate risk, allowing for a richer quantification of climate model ensemble uncertainty. Here, we further analyse the propagation of hazard, exposure and vulnerability uncertainties by varying a number of input factors based on a discrete, scientifically justified set of options. We explore the uncertainty and sensitivity of risk to these variations, using the PAWN (PiAnosi and WagNer) method for global sensitivity analysis, allowing for an attribution of uncertainty to different drivers of the total uncertainty budget. We demonstrate the approach through an application to assess heat-stress risk to outdoor physical working capacity in the UK. In this application, we demonstrate how the risk estimated across plausible input settings better captures uncertainty and extreme outcomes (important for decision making); that all uncalibrated/non-bias-adjusted climate data sources underestimate risk in the recent past (highlighting the need for data calibration); and that when a global warming level framing is used it is the choice of global warming level that this risk is most sensitive to (2 °C or 4 °C warmer than pre-industrial), particularly in the south of the UK. This highlights the importance of mitigating climate change to reduce heat-stress risk.

E-mail address: laura.dawkins@metoffice.gov.uk (L.C. Dawkins).

https://doi.org/10.1016/j.crm.2023.100511
Received 13 January 2023; Received in revised form 14 April 2023; Accepted 14 April 2023
Available online 28 April 2023

1. Introduction

The climate is changing, causing irreversible damage to our planet (IPCC, 2022). The water cycle is intensifying, bringing more intense rainfall and associated flooding, as well as more intense drought in many regions (IPCC, 2021); populations and livestock exposed to extreme heat are increasing, exacerbated in cities by the urban heat island effect, leading to increased morbidity and mortality (World Health Organisation, 2022); and new global annual records have been set for the highest insured losses mainly due to payouts related to three major hurricanes in the USA (Harvey, Irma, and Maria), wildfire outbreaks in California, and many thunderstorms, windstorms, and other severe weather events around the world (Aznar-Siguan and Bresch, 2019). The UK experienced an unprecedented extreme heatwave in July 2022, with temperatures reaching 40.3 °C in Coningsby (Lincolnshire), and exceeding 37 °C for a large part of England. This heat brought challenging conditions for care services supporting the elderly and vulnerable, with an increase in heat related deaths, and these conditions are projected to increase in frequency and severity with climate change (Hanlon et al., 2021; Arnell et al., 2021).

In order to understand and adapt to climate change it is important to quantify the future change in risk, rather than the hazard alone. The Intergovernmental Panel on Climate Change (IPCC) definition of risk combines information about the hazard (e.g. extreme temperature during a heatwave), exposure (e.g. the location and number of people exposed) and vulnerability (e.g. the susceptibility of those exposed) to compute metrics necessary for assessing risk (e.g. mortality), and has been widely used to inform future climate risk (e.g. Roy et al., 2021; Viner et al., 2020; Sharma and Ravindranath, 2019; Simpson et al., 2021).

Open-source quantitative risk assessment frameworks, such as the CLIMADA platform (Aznar-Siguan and Bresch, 2019), allow for the IPCC definition of risk to be applied in a spatially consistent way to a wide range of hazards (e.g. tropical cyclones, flooding, heatwaves) to assess current and future risk, quantified in a range of ways (e.g. financial risk, mortality, labour productivity etc.). For example, Lüthi et al. (2021) use the CLIMADA platform to model the economic risk associated with wildfires in a globally consistent way; Gettelman et al. (2018) use the platform to quantify future cyclone risk based on high resolution global climate model data; and Stalhandske et al. (2022) use CLIMADA to quantify future heat related risk in terms of mortality and labour productivity across Switzerland.

Carrying out such risk assessments requires a number of subjective choices to be made about how the hazard, exposure and vulnerability are captured. Hence, as well as translating hazard into risk, transparent and robust climate risk assessments, and subsequent adaptation decision making, must take into account and explore the many inherent uncertainties in the process. This can help to identify a wider range of plausible outcomes, important for decision making, and can focus future research, to better quantify those inputs that matter most for reducing uncertainty in the output. Here we explore this within the setting of the UK, but a similar approach could be applied to other regions. This follows on from a number of studies in the UK on characterising and exploring uncertainties in impact assessments, predominantly applied to the water sector. For example, Dessai and Hulme (2007) present an assessment framework that allows the identification of water resource management adaptation strategies that are robust to climate change uncertainties in the East of England, and New et al. (2007) explore the implications of a probabilistic end-to-end risk-based framework for climate impacts assessment, for the Thames River, UK.

When considering the hazard, for example, there are a number of different sources of climate projections, such as (for the UK) UKCP18 (Lowe et al., 2018), CMIP6 (Haarsma et al., 2016) and Euro-CORDEX (Jacob et al., 2014). These different sources can provide different projected changes in the meteorological conditions and have different responses to greenhouse gas emissions, due to their differing model structures and parametrisations. Additionally, the future level of emissions is unknown, depending heavily on the policies made and actions taken by governments throughout the world (Betts and Brown, 2021), requiring the exploration of different scenarios leading to different global warming levels. Furthermore, the actual realisation of climate for a particular time window is subject to internal variability, necessitating the consideration of multiple alternative realisations (i.e. ensemble members). In addition, because climate models are *models*, and hence are imperfect representations of reality, they require calibration (such as bias correction or application of change factors) to reduce systematic biases. Note, however, that calibration can only take us so far and there remains a place for expert judgement in interpreting the models (Thompson and Smith, 2019). This calibration is an additional source of uncertainty, as different approaches will lead to differences in the resulting data (Ho et al., 2012).

As well as the uncertain hazard component, the exposure and vulnerability are uncertain. For example, the way in which populations will migrate and grow in future years is unknown, and the way in which people/assets/ecosystems are impacted by a hazard (i.e. the vulnerability) is often estimated based on limited data which is unlikely to capture all circumstances. As such, alternative representations of each component must be considered to understand the uncertainty and sensitivity of risk to varying these inputs over some plausible range, using insights such as the shared socio-economic pathways developed by Riahi et al. (2017), which characterise a number of plausible population narratives for the coming century.

Different methods for carrying out uncertainty and sensitivity analysis (U&SA) have been proposed in the scientific literature. Sensitivity analysis provides information on the relative importance of model inputs and assumptions (Saltelli et al., 2019). It allows us to ask questions such as 'Which components of the risk modelling chain (i.e. hazard, exposure and vulnerability) is risk most sensitive to?'. This is distinct from uncertainty analysis, which addresses the question 'How uncertain is the output (risk) when considering plausible inputs?'. In practice, these analyses commonly follow the approach of repeatedly running the model against different values of the uncertain input factors (i.e. hazard, exposure, vulnerability). Often both uncertainty and sensitivity analysis are carried out by varying each input one-by-one (keeping all other inputs fixed). Saltelli et al. (2019) discuss the shortcomings of such an approach, including how regions of possible input space are excluded, and instead advocate a 'global' approach. In a global analysis, all inputs are varied together, ensuring a range of relevant combinations of the input space are used, subsequently assessing further output uncertainty and sensitivity. Note of course that this does not ensure all parts of solution space are covered, as this will depend on the

selection of inputs considered.

Quantitative risk assessment frameworks such as CLIMADA (Aznar-Siguan and Bresch, 2019) provide a useful tool for carrying out global U&SA, as they can be repeatedly applied with minimal computational expense. Kropf et al. (2022) present an extension of the CLIMADA platform that seamlessly integrates the SALib – Sensitivity Analysis Library in Python package (Herman and Usher, 2017) into the overall CLIMADA modelling framework, via the UNcertainty and SEnsitity QUAntification (unsequa) module. Following similar steps as a generic U&SA (Pianosi et al., 2016), their approach requires the specification of a probability distribution for each of the uncertain input factors (e.g. input data and parameters related to the hazard, exposure and vulnerability components); samples from these distributions to generate plausible alternative inputs; uses all combinations of inputs (i.e. a global approach) to calculate risk using the CLIMADA platform; and uses the SaLib package to calculate sensitivity indices, i.e. indices that quantify the relative importance of each uncertain input factor with a number varying between 0 and 1. In some cases the definition of an input factor probability distribution may be relatively straightforward, e.g. when the underlying statistical model for the input factor has been derived within the study allowing for a quantification of uncertainty. However, as noted by Kropf et al. (2022), when this information is not available it is often not evident how to perturb the inputs, and in particular it is difficult to define physically consistent statistical perturbations of geospatial data.

In this study we present an alternative approach for carrying out U&SA using the CLIMADA platform. Rather than specifying probability distributions for the input factors, we define a discrete set of scientifically justified inputs. For example, when representing the uncertainty in the hazard component, we define different inputs as different discrete climate data sources (e.g. UKCP18, CMIP6 and Euro-CORDEX) each of which has been assessed as plausible by different climate modelling centres or inter-comparison projects. In doing so, we make no assumption about which input selections are more or less likely, but instead define the results in terms of the uncertainty/sensitivity across these discrete settings. We then use the PAWN sensitivity analysis approach of Pianosi and Wagener (2015) (as implemented in the SAFE toolbox (Pianosi et al., 2015)) to calculate and visualise the sensitivity indices. This approach still relies on expert judgment in terms of defining the discrete set of plausible inputs, and as is common in U&SA, the results will depend greatly on this definition (Pianosi et al., 2016; Kropf et al., 2022). This is discussed further in Section 4.

To provide a richer quantification of uncertainty, rather than using the CLIMADA platform directly (as in Kropf et al., 2022), our approach applies the extended CLIMADA framework developed by Dawkins et al. (2023). This novel extension of the platform retains and provides a richer quantification of climate model ensemble (aleatoric) uncertainty by using statistical techniques to model and stochastically simulate alternative realisations of climate risk (described in more detail in Section 2.1).

We demonstrate this approach through the same application as in Dawkins et al. (2023), which focuses on the risk of reduced outdoor physical working capacity in the UK as a result of extreme heat and humidity. Specifically, climate risk is represented by the expected number of days of physical outdoor work lost in an average year due to heat-stress. With our U&SA, we answer four key uncertainty and sensitivity analysis questions:

1. How does risk compare when estimated using different hazard data sources?
2. How uncertain is risk when considering all plausible inputs (that is, when varying not only hazard source but also exposure and vulnerability)?
3. What is the relative sensitivity of risk to the components of the risk modelling chain (i.e. hazard, exposure and vulnerability)?
4. How does this sensitivity vary in space, across the UK region?

Questions 1 and 2 are important for understanding the range and variability in plausible outcomes, which may be relevant for adaptation decision making (for example to avoid a plausible extreme outcome). Here we consider questions 1 initially (focusing just on the hazard data source component), so as to identify which data sources provide plausible outcomes for consideration in the following three questions. Questions 3 and 4 are important for informing future research focus (to constrain the most sensitive parts of the system), and possible best approaches for minimising risk. For example, if risk is most sensitive to the future population scenario used, this suggests a possible approach for adaptation is to take socio-economic measures to minimise the likelihood of high risk scenarios, and future research should focus on narrowing the uncertainty associated with this input.

We hope our study will provide a blueprint for other risk modellers to analyse the impacts of discrete modelling choices in a coherent and structured way, as well as a demonstration of the importance of doing such analysis. Although our paper is mainly intended for modellers, it can also be relevant for users of risk model outputs, by demonstrating the importance and value of having uncertainty and sensitivity information along with risk estimates.

Section 2 presents the material and methods used and developed in this study: the extended CLIMADA platform for assessing climate risk, our approach to quantify uncertainty and sensitivity of risk estimates, and a description of the discrete modelling choices analysed here for the hazard, exposure and vulnerability components. Section 3 presents and discusses application results for the UK heat-stress example. A discussion of the limitations of the study is included in Section 4 and of the implications for risk management and decision making in Section 5.

2. Material and methods

2.1. Assessing climate risk

This study builds upon the risk assessment framework of Dawkins et al. (2023), to explore the uncertainty and sensitivity of risk when varying the inputs of the assessment. This framework assesses risk based on a climate model ensemble and uses statistical

modelling techniques to provide a richer quantification of the climate model ensemble uncertainty.

Within this framework, CLIMADA, an open-source probabilistic event-based risk assessment platform (Aznar-Siguan and Bresch, 2019), is used to estimate risk based on each climate model ensemble member. For this, the hazard is defined as a set of weather events described in terms of their physical intensity/magnitude, and their probability of occurrence; the exposure is defined as the location and value of relevant people and/or assets; and the vulnerability is quantified via functions representing the sensitivity of the exposed people/assets to the hazard. The risk is then estimated as:

$$\text{Risk} = \text{Probability} \times \text{Severity}, \tag{1}$$

$$\text{Severity} = \text{Exposure} \times f_{vuln}(\text{HazardIntensity}), \tag{2}$$

where f_{vuln} is the vulnerability function. An additional advantage of such frameworks is that this calculation is made consistently across space, i.e. capturing all relevant locations in space coherently together. This is particularly relevant for stakeholders with spatially distributed assets, located across a country or region. While the functionality of CLIMADA is growing, there are some limitations in its usage including the need for Python coding skills, and other open-source tools are also available for this type of assessment (e.g. RiskScape (Paulik et al., 2022)).

Climate models are imperfect representations of the climate system and hence uncertainty in the future hazard arises in many ways. One such uncertainty is in the realisation of the climate for a particular time window, which is subject to internal variability (aleatoric uncertainty). To help quantify this uncertainty, climate projections often comprise a number of ensemble members. However, climate models are very computationally expensive to run, hence there is often a limit to the number of ensemble members that can be produced and subsequently a limited quantification of uncertainty across these ensemble members. To help to overcome this, the framework of Dawkins et al. (2023) uses a Generalised Additive Model (GAM) to statistically model risk across space, representing all ensemble members in combination, while taking into account the differences between them. Once fitted, this statistical model can be used to sample many more realisations of risk, representative of a larger collection of plausible ensemble members, providing a richer quantification of the aleatoric uncertainty in risk. See Dawkins et al. (2023) for more detail. This framework is shown in Fig. 1, highlighting the five categories of inputs that must be specified in order to carry out a climate risk assessment. Namely, the hazard data source (e.g. UKCP18); the calibration method (e.g. bias correction); the global warming level (i.e. the future time slice of the hazard data used from different emissions scenarios, see Section 2.5); the UK Shared Socio-economic pathway (SSP, i.e. the future projected exposure/population statistics, see Section 2.6); and the form of the vulnerability function (i.e. the parameters of the function). These are the inputs that will be varied within the uncertainty and sensitivity analysis presented in this study (see Sections 2.3–2.7).

The subsequent output of the end-to-end framework is a representation of the probabilistic predictive distribution of risk (spatially

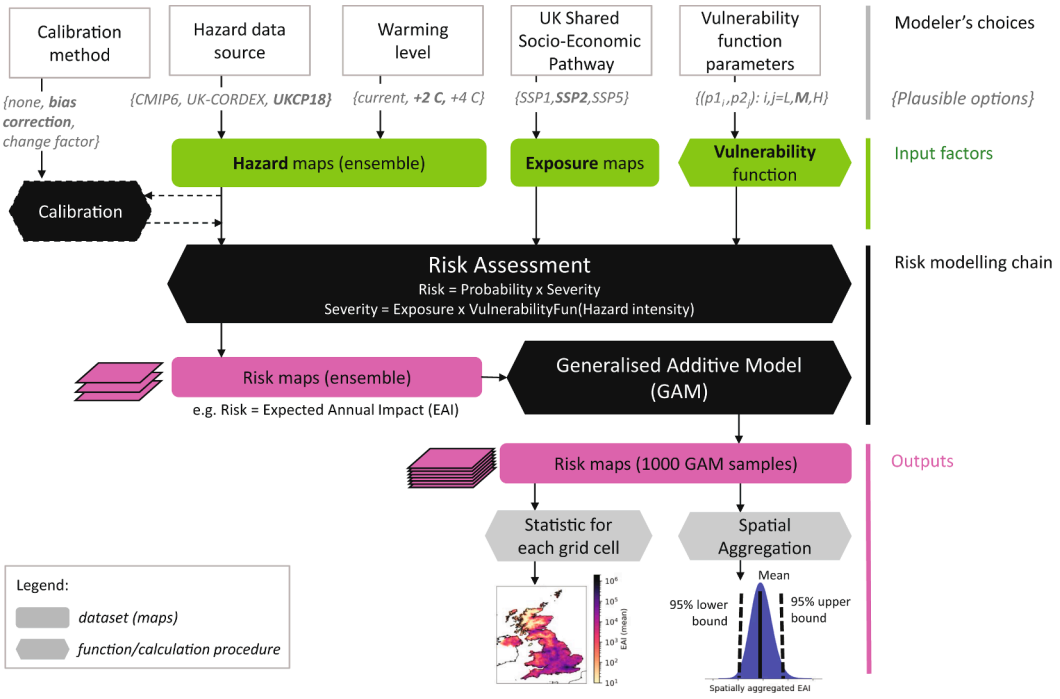

Fig. 1. A schematic demonstrating the climate risk assessment modelling chain, the modeler's choices associated with the model input factors, and the resulting outputs explored in this study. For each input factor, the choices in bold are the ones used for the baseline case of Section 3.1. The range of choices for each input factor are described in detail in Sections 2.3–2.7. In particular, the vulnerability function parameters (p_1 and p_2) each take three values, a mean value (M), a lower value (L) and an upper value (U).

coherently at each location in the region (Dawkins et al., 2023)). In practice, this is quantified using 1000 samples of risk from the fitted GAM. These samples can be used to represent the full predictive distribution of risk or quantify any statistics of it, such as the mean or the 95% prediction interval (i.e. the uncertainty in the predicted risk). In addition, the risk can be considered for each location or aggregated over space to represent a given region.

As described in the introduction, within this study we demonstrate the quantification of risk and subsequent U&SA through an application focusing on the risk of reduced outdoor physical working capacity in the UK as a result of extreme heat and humidity. Hence, for a given set of inputs (hazard data source, calibration method, warming level, UK SSP, vulnerability function) the predictive distribution of risk is estimated in each location (grid cells covering UK land), where risk is the expected annual total number of days of physical outdoor work lost due to heat-stress (conditional on the selected inputs). See Section 3.1 for a demonstration of this risk quantification using the modeler's choices highlighted in bold in Fig. 1.

2.2. Uncertainty & sensitivity analysis

Within this study we aim to demonstrate an approach for extending the CLIMADA based risk assessment framework of Dawkins et al. (2023) to assess the uncertainty and sensitivity of risk to the input factors associated with the hazard, exposure and vulnerability.

As described in the introduction, rather than varying each input factor by sampling a set of additive/multiplicative perturbation factors (as in the inbuilt CLIMADA functionality Kropf et al., 2022), here we define our input variability space based on a discrete selection of scientifically justified choices of input datasets. That is, we select a range of inputs that span those considered to be plausible by the scientific community, for example using exposure data from a selection of future population projections (SSPs). We do this because, in practice, it is very challenging to define all input uncertainties using a set of perturbation factors. Also, by using a discrete set of plausible choices for the inputs, we can directly relate our output back to the specific combinations of inputs used to generate it. In addition, we make no assumption about which input combinations are more or less likely, but instead define the results in terms of the uncertainty/sensitivity across these discrete settings that are explored. The input settings used in this analysis are described in detail in Sections 2.3–2.7.

Based on these input factor settings, we then demonstrate an approach for answering two Uncertainty Analysis questions: (1) How does risk compare when estimated using different hazard data sources? (2) How uncertain is risk when considering all plausible inputs? And two Sensitivity Analysis questions: (3) What is the relative sensitivity of risk to the components of the risk modelling chain (i.e. hazard, exposure and vulnerability)? (4) How does this sensitivity vary in space, across the UK region?.

To address question 1, we use the end-to-end risk assessment framework (Fig. 1)) to estimate risk using a number of different climate data sources, keeping the other components (exposure and vulnerability) constant. The subsequent predictive distributions of risk derived from each data source are then compared.

To address question 2, we apply the end-to-end risk assessment framework for all plausible discrete settings, that is, all combinations of plausible choices for the hazard, exposure and vulnerability input factors. In doing so, we are essentially placing a uniform categorical distribution on each input factor and exploring the input space exhaustively. The uncertainty in risk across all of these settings is then presented both spatially (as the standard deviation of the overall predictive distribution of risk), and when aggregated over space (as the full distribution of risk across the input settings).

To address questions 3 and 4, the same set of inputs are exhaustively varied and the sensitivity of risk to these variations is explored using a formal global sensitivity analysis approach known as PAWN (Pianosi and Wagener, 2015; Pianosi and Wagener, 2018). PAWN is a distribution-based method, meaning that the sensitivity of the model output is measured in terms of the changes induced in the whole output distribution created when evaluating the model at various input settings, as opposed to variance-based approaches which only use moments of the output sample (Saltelli et al., 2010).

Specifically, the PAWN method characterises the sensitivity of the model output to a given input factor (e.g. warming level), as the distance between the unconditional empirical Cumulative Distribution Function (CDF) of the output across all input values, and the conditional empirical CDF of the output when that input is fixed and all other inputs are allowed to vary. This measure is known as the Kolmogorov–Smirnov (KS) statistic. When this difference is large for a given input, the KS statistic is large, representing how the output is highly sensitive to that input. Hence, comparing this statistic across input factors allows for a comparison of the relative sensitivity of the outputs to the inputs. Within this study, the KS statistic is compared for spatially aggregated risk (to address question 3), and for risk at each location (to address question 4).

To produce sensitivity indices with the PAWN method (or any other global SA method (Pianosi et al., 2016)) we are required to define a 1–2-1 mapping between the model's inputs and the output. However, when applying the risk assessment framework used in this study (Dawkins et al., 2023), one input factor combination maps to the full predictive distribution of risk (i.e. not a 1–2-1 mapping). Hence, when carrying out the sensitivity analysis we must define a specific summary statistic of the predictive distribution of risk to create such a 1–2-1 mapping, e.g. using the mean or a quantile of the distribution. To ensure that this richer uncertainty quantification is not lost, here the sensitivity analysis will be applied to both the mean and the upper and lower tails of the predictive distribution of spatially aggregated risk (as shown in the 'Spatial Aggregation' output in Fig. 1).

2.3. Defining inputs: hazard data source

The physical intensity of the hazard is quantified using the heat-stress metric 'Humidex', calculated from gridded temperature and relative humidity data based on the approach of Masterton and Richardson (1979) and Rana et al. (2013):

$$\text{Humidex} = T + \frac{5}{9}\left(\left[6.112 \times 10^{\left(\frac{7.5T}{237.7+T}\right)} \times \frac{Rh}{100}\right] - 10\right), \tag{3}$$

where T is temperature (at a given location and time), and Rh is the corresponding relative humidity. Specifically, here, similar to Dawkins et al. (2023) and Strauss et al. (2021), each day in the data record is considered to be an 'event'. Due to the lack of availability of hourly variables in most climate data sets, the daily maximum temperature at the Earth's surface and daily mean relative humidity are used in Eq. 3 to represent Humidex on each day.

The various datasets used within this study to characterise the heat-stress hazard are summarised in Table 1, and described in more detail in the Supplementary Material. For each, data over the UK land region is used and transformed to the HadUK-Grid 12 km grid, on the British National Grid projection (EPSG:27700), using linear interpolation. These three climate projection data sources (UKCP18, UK-CORDEX and CMIP6 HighResMIP) are used because they represent the current state-of-the-art and they sample a range of climate uncertainty. Namely, both parameter uncertainty, through the use of the UKCP18 Purturbed Parameter Ensemble (PPE), and structural uncertainty, through the use of the multi-model ensembles UK-CORDEX and CMIP6 HighResMIP (see Section 1 of the Supplementary Material for more detail). The DePreSys4 hindcast is included to represent a richer representation of climate variability within the historical period. and HadUK-Grid and ERA5 are used to represent the 'true' observed historical period, as the current state-of-the-art in gridded observation datasets (again, see Section 1 of the Supplementary Material for more detail).

To address question 1 in Section 2.2 (How does climate risk compare when estimated using different hazard data sources?) the risk assessment framework is applied to each of these datasets. To provide a historical 'truth' for comparison the same framework is applied to historical observations and reanalysis. Specifically, HadUK-Grid is used to represent observed daily maximum temperature and ERA5 is used to represent observed daily mean relative humidity (due to a lack of high altitude relative humidity data in the HadUK-Grid product). These datasets are used as they are the current state-of-the-art in gridded observation products (see Section 1 of the Supplementary Material for more detail).

In addition, within this data source comparison, a selection of calibration approaches are compared. In all cases these are applied to just the UKCP18 RCM dataset (due to the time limitations of the study), with the same combination of HadUK-Grid and ERA5 used as historical 'truth' within each approach.

2.4. Defining inputs: calibration method

When using climate model data for impact studies such as this, where absolute values rather than relative changes are explored, it is recommended that the data be calibrated to ensure the severity and frequency of impactful events are accurately captured (Met Office, 2018; Ho et al., 2012). It should, however, be noted that calibration can only go so far in addressing model limitations (Thompson and Smith, 2019), and indeed may lead to physical inconsistencies in the data (Ehret et al., 2012; Sippel et al., 2016).

As described by Ho et al. (2012), various calibration methods have been used in climate change studies, generally falling into two distinct categories: 'bias correction' and 'change factor'. However, few published studies carefully investigate the sensitivity of their results to the choice of calibration method. Ho et al. (2012) provide one such comparison, applied to climate projections of European daily surface air temperatures, and find that the two calibration strategies give substantially different spatial patterns of warming. Similarly, here we present the comparison of two different calibration approaches applied to the UKCP18 climate projections. In all cases, similar to Ho et al. (2012) and Garry et al. (2021), calibration is applied separately to each grid cell and to each variable.

Using a similar notation to Ho et al. (2012), suppose X_0 represents the historical observations, and X_c and X_c' climate model projections in the historical and future periods respectively. The aim of calibration is to achieve an estimate of future observations, X_0'.

Bias correction

The bias correction strategy assumes that the model discrepancies stay constant in time. That is, the relationship (bias) between X_0

Table 1
Overview of datasets used in this study. RCM = Region Climate Model, GCM = Global Climate Model, PPE = Perturbed Parameter Ensemble.

Dataset	Number of ensemble members	Horizontal spatial resolution	Temporal coverage	Reference(s)
UKCP18 RCM	12 member PPE	~12 km	1981–2080 (daily)	Murphy et al. (2019)
UK-CORDEX	59 different	~12 km	1981–2080 (daily)	Jacob et al. (2014)
(derived from Euro-CORDEX)	RCM-GCM combinations			Barnes et al. (2022)
CMIP6	4 different models	~50 km	1950–2050 (daily)	Haarsma et al. (2016)
(HighResMIP) DePreSys4	10 hindcasts	~60 km	1960–2019 (daily)	Thompson et al. (2017)
HadUK-Grid	N/A	~12 km	1960–2018 (daily)	Hollis et al. (2019)
ERA5	Ensemble not used here	~30 km	temperature only 1979–2018 (daily) relative humidity only	Hersbach et al. (2020)

and X_c in the historical period, is the same in the future, i.e. between X'_0 and X'_c. This allows for estimates of future observations to be obtained by mapping from future model data (X'_c) to future observations (X'_0) based in the relationship between historical observations (X_0) and climate model (X_c). This relationship (bias) is therefore first quantified and then used to apply this mapping.

In the case where a distribution mapping bias correction is applied, this mapping can be summarised as:

$$X'_0 = F_0^{-1}(F_c(X'_c)), \tag{4}$$

where $F_c(\cdot)$ is the cumulative distribution function (CDF) of X_c (historical model), and F_0^{-1} is the inverse CDF (also known as the quantile function) of X_0 (historical observations).

Here, bias correction is applied to daily maximum temperature and daily mean relative humidity, separately for each climate model ensemble member, each variable and each grid cell in the UK, using HadUK-Grid and ERA5 to represent historical observations for temperature and relative humidity respectively. Each calendar month is calibrated separately, using a historical base period 1998–2017.

Similar to Garry et al. (2021), here the Scaled Distribution Mapping (SDM) approach of Switanek et al. (2017) is used. This bias correction method is conceptually similar to Quantile Delta Mapping (Cannon et al., 2015), but more explicitly accounts for the likelihood of individual events (i.e. recurrence intervals). In addition, the approach preserves any trend in the data by first de-trending that data, and then adding the trend back to the corrected data at the end of the process. SDM has been shown to perform as least as well as other approaches (Switanek et al., 2017), and Garry et al. (2021) showed an improvement in the UKCP18 representation of temperature and relative humidity data relative to observations when using this approach. As described above, this bias correction approach is applied to each variable and each grid cell separately and is hence a univariate bias correction approach. As such, there is the potential for introducing some spatial incoherence in the resulting field and a physical inconsistency between different variables, a common potential issue with bias correction approaches. The validity of the approach applied, here to UKCP18 RCM data, is explored by Garry et al. (2021) within in their supplementary material. They provide evidence that this univariate bias correction approach improves the representation of the spatial pattern of dependence between the temperature and humidity data relative to observations when compared to the raw model data and hence conclude that this gives confidence in using this approach. They do, however acknowledge that, depending on whether the underlying model is biased in the dependence structure, multivariate techniques may be more appropriate. Further exploration of this is beyond the scope of this paper but is an important consideration for future applications.

Change Factor

Alternatively, the change factor strategy assumes that the change from present-day to future in the observations is consistent with the equivalent change in the climate model between these two time periods. This allows for estimates of future observations (X'_0) to be obtained by mapping historical observations (X_0) into the future, based on the relationship between historical and future climate model data (X_c and X'_c respectively).

This mapping can be summarised as:

$$X'_0 = F_{c'}^{-1}(F_c(X_0)), \tag{5}$$

where $F_c(\cdot)$ is the CDF of X_c (historical model), and $F_{c'}^{-1}$ is the inverse CDF (quantile function) of X'_c (future model).

As in the bias correction approach, the change factor approach is applied to daily maximum temperature and daily mean relative humidity, separately for each climate model ensemble member, each variable, month-of-the-year and grid cell in the UK, using HadUK-Grid and ERA5 to represent historical observations for temperature and relative humidity respectively. Rather than applying to a continuous future period and accounting for the temporal trend (as in the SDM bias correction approach), this simple change factor approach assumes stationarity in time, and hence is applied separately for different future periods of interest. Here these are future periods representative of 2 °C and 4 °C global temperature increase beyond pre-industrial (see Section 2.5).

Similar to Ho et al. (2012), the distributions (and hence CDF and inverse CDF) of X_c and X'_c are represented by a Normal distribution and the mean (μ) and standard deviation (σ) are calculated empirically. This does not assume that the data to be calibrated is Normally distributed. If this is not the case, the data is first transformed to Normal before applying the calibration. The mapping between distributions, as shown in Eq. (5), is achieved by adjusting for the differences in the means and standard deviations between the distributions of X_c and X'_c. That is, for each climate model (UKCP18) ensemble member, each variable (daily maximum temperature and daily mean relative humidity), each month of the year (e.g. January, February etc.), each warming level representative time period (2 °C and 4 °C) and each grid cell:

$$X'_0 = \mu'_c + \frac{\sigma'_c}{\sigma_c}(X_0 - \mu_c), \tag{6}$$

where μ_c and μ'_c are the empirical mean of X_c and X'_c respectively, and σ_c and σ'_c are the equivalent empirical standard deviations of X_c and X'_c respectively.

Here, the two variables to be calibrated are temperature and relative humidity. Temperature data is very commonly represented by a Normal distribution, and exploratory analysis of the data (not shown) indicated this to be suitable here. Since relative humidity is a strictly positive variable, the logit transformation is applied, and the change factor calibration is applied to the resulting Normally distributed transformed variable. After applying the change factor, the variable is then back transformed to the relative humidity scale.

2.5. Defining inputs: warming level

Consistent with CCRA3 guidance (Betts and Brown, 2021), three different global warming levels are considered here: current/recent past, and 2 °C and 4 °C increase in global mean temperature beyond the pre-industrial level. Similar to many examples (Garry et al., 2021; Hanlon et al., 2021; Nikulin et al., 2018; Iturbide et al., 2021; F. et al., 2016), here a time slice approach is used to identify periods that represent each warming level. Specifically, here this follows the IPCC approach which allows for the time window to be reached at any point within the data record.

In all cases, the current climate (recent history) is represented by the period 1998–2017. For the 2 °C and 4 °C above pre-industrial warming levels, a similar approach to that used in the Intergovernment Panel on Climate Change (IPCC) interactive atlas, as described by Nikulin et al. (2018), is used. The year when the given level of warming is reached is found for each climate data source and each ensemble member (based on the driving global model simulation) from a moving 21-year mean of global temperature anomaly. This year is then used as the central estimate for defining the future period (9 years prior and 10 years post). In cases where less than 15 years of data are available to represent a given warming level, that ensemble member is not included in the analysis. In all cases this is based on non-bias corrected global simulations.

Here, the central years are taken from the analysis of Hanlon et al. (2021) for UKCP18, and Iturbide et al. (2021) for the UK-CORDEX (CMIP5) and CMIP6 ensembles. The representative time slices for each ensemble member, data source and warming level are given in Table 1 of the Supplementary Material, including references to where this information can be obtained. The 2 °C and 4 °C warming levels are used in the uncertainty and sensitivity analysis within this study to represent plausible future warming levels, justified by CCRA3.

2.6. Defining inputs: shared socio-economic Pathways

In climate risk and resilience research it is important to consider both future scenarios for the climate and the economy, since both affect society's ability to manage and cope with climate risks (Stenning et al., 2021). Similar to Dawkins et al. (2023), here a scenario modelling approach is used to characterise how society and the economy may evolve into the future. Specifically, three of the IPCC Shared Socio-economic Pathways (SSPs) are considered within the uncertainty and sensitivity analysis (O'Neill et al., 2015):

- SSP1: Sustainability (Taking the Green Road)
- SSP2: Middle of the Road
- SSP5: Fossil-fuelled Development (Taking the Highway)

These global IPCC SSPs have been used to develop a consistent set of SSPs specifically for the UK (Harmackova et al., 2022). As part of this project, a set of quantified projections for specific indicators (e.g. population density) at appropriate temporal and spatial resolutions (ranging from a 1 km grid to the whole of the UK) have been produced (Merkle et al., 2022). This representation of the SSPs is used within this study.

Specifically, SSP2 captures a future in which medium challenges to mitigation and adaptation are experienced (Kriegler et al., 2014), and future trends do not differ substantially from the historical social, economic and technological patterns. This is the SSP used in Dawkins et al. (2023) in the demonstration of the risk framework described in Section 2.1. For comparison, SSP1 is used to represent a future in which the UK shifts to a more sustainable system as a result of increased environmental pressure. This represents a scenario with low challenges in terms of mitigation and adaptation. Conversely, SSP5 is included to represent a future with high challenges to mitigation. In this SSP, low public support in sustainable development hinders sustainable transformation, and large sources of shale gas are discovered and used in the UK, increasing urbanisation in Scotland and in cities throughout the UK. It should be noted, of course, that these quantified SSPs represent only a small number of possible futures, and many alternatives are possible. As such, it is very unlikely that we will follow one of the quantified SSPs in the real world. That is, they are not a prediction but a useful guide for exploring plausible future societies.

The UK SSP quantified projections include many indicators such as population, urbanisation and employment. The application presented in this study aims to quantify the impact of heat stress on outdoor physical working capacity in the UK. Hence, here we use the 'employment' indicator to capture information about the number of people working across the UK. In particular, those relating to outdoor physical jobs (e.g. construction and agriculture) are obtained and summed together to represent the total exposure in each location. In this application, similar to Dawkins et al. (2023), the 12 km version of the quantified projections are used, to align with the horizontal spatial resolution of the hazard data.

This 'employment' indicator is available for each year in the range 2020–2100. To isolate the sensitivity to varying the SSP *scenario* within the U&SA presented in this study, a specific year is selected, and held constant, to represent each warming level (current, 2 °C and 4 °C). As in Dawkins et al. (2023), for the 'current' warming level the year 2020 is used, and for the 2 °C and 4 °C warming levels, results from the IPCC Sixth Assessment Report (AR6) are used. In AR6, time periods are identified over which these two global warming levels are crossed, based on multiple lines of evidence (see Table 4.5 in Chapter 4 of the IPCC AR6, IPCC, 2021). As in Dawkins et al. (2023), the year 2041 is used for the 2 °C warming level and 2084 for the 4 °C warming level (see Dawkins et al. (2023) for further discussion of this). Fig. 2 provides a graphical representation of the difference between these exposure input settings used within the uncertainty and sensitivity study. These show how UK SSPs 1 and 2 are largely consistent in the number of people working in outdoor physical jobs (although slightly less in SSP1), whereas SSP5 sees much larger numbers, particularly in the future year used to represent the 4 °C warming level. This increase is particularly large in already highly populated places, and in Scotland, consistent

with the SSP5 storyline related to the discovery of a large source of shale gas in Scotland.

As discussed in Dawkins et al. (2023), the uncertainty of the risk to the timing of warming levels, representative of the climate sensitivity of the climate model, should also be explored (i.e. the choice of year to represent each warming level within the SSP data). To address this within this study, we carry out an additional sub-analysis varying this input variable while keeping the SSP fixed. We do this separately because varying both SSP and the warming level year together in a global U&SA would result in highly implausible combinations (e.g. SSP1 [sustainability], 4 °C warming level, and warming level year 2032). For this sub-analysis, the SSP is held constant at SSP5. This SSP is chosen because the date ranges over which each of the warming levels (2 °C and 4 °C) is reached for RCP8.5 model projections can be obtained from Table 4.5 in Chapter 4 of the IPCC AR6, IPCC (2021). For each warming level, the date ranges in this table are used to define a lower, middle and upper year, namely (2032, 2041, 2051) for the 2 °C warming level, and (2075, 2084, 2094) for the 4 °C warming level.

2.7. *Defining inputs: vulnerability function parameters*

The vulnerability function captures the relationship between the hazard and the impact this has on the exposed people/assets. This function is often defined in terms of a number of parameters, which must be estimated based in relevant available impact data, and specified within the risk assessment.

For the application considered in this study, we require a vulnerability function that captures the relationship between the Humidex heat stress index and the impact this has on physical working capacity. For this, as in Dawkins et al. (2023), we use the function of Foster et al. (2021), derived based on 338 work sessions in climatic chambers (low air movement, no solar radiation) spanning mild to extreme heat stress:

$$\text{Physical Working Capacity}(\%) = \frac{100}{1 + \left(\frac{p_1}{\text{Humidex}}\right)^{p_2}}, \tag{7}$$

where p_1 represents the value of Humidex that elicits 50% physical working capacity, estimated to be 54.5 °C (with upper and lower 95% confidence interval limits of 55.79 °C and 53.78 °C respectively); and p_2 represents the gradient of the vulnerability function (i.e. the increment of decreased physical working capacity per °C increase in Humidex), estimated as −4.1%/°C (with upper and lower 95% confidence interval limits of −4.597%/°C and −3.804%/°C respectively). This function is inverted to relate Humidex to the 'impact' on physical working capacity (i.e impact = 1 - physical working capacity), and scaled to the impact range 0–1 by dividing by 100. The resulting function has a sigmoidal form, as can be seen in Fig. 2 (e). Ideally, the vulnerability function should vary across the spatial and temporal domain to capture how this relationship may differ across demographics (e.g. age), location and time. Here, however, due to the limited research in this area for the UK, we apply the same function throughout space and time, thus ignoring those differences. Future research should aim to improve upon this representation of vulnerability. For the U&SA, the parameters of this vulnerability function are varied (by the same amount in all locations). This is done based on the upper and lower 95% confidence

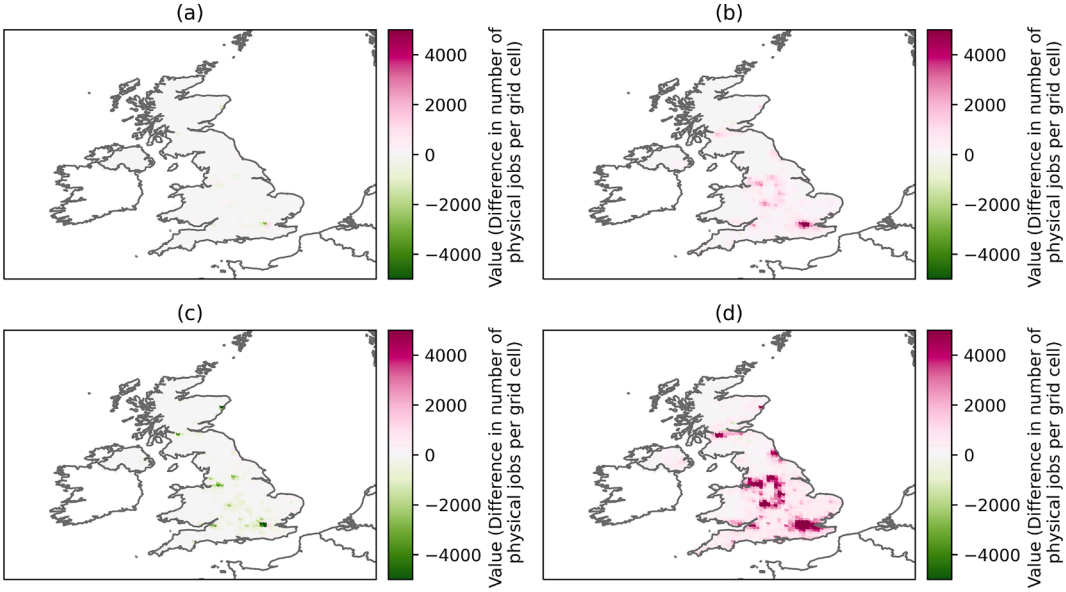

Fig. 2. A graphical representation of the difference between the exposure input settings used in our uncertainty and sensitivity study. The maps show the difference in the number of people working in outdoor physical jobs between SSPs, specifically: (a) SSP1 - SSP2 in the 2 °C warming level year 2041; (b) SSP5 - SSP2 in the 2 °C warming level year 2041; (c) SSP1 - SSP2 in the 4 °C warming level year 2084; and (d) SSP5 - SSP2 in the 4 °C warming level year 2084.

interval limits described above, providing a high, medium and low value for each parameter. The variability in the vulnerability function as a result of varying these parameter can be seen in Fig. 3. Basing these choices of vulnerability function parameter settings on the modelling results of Foster et al. (2021) provides some meaning to the range of values tested. They are, however, only representative of the statistical uncertainty in the model fitted to the data in Foster et al. (2021). As such, the uncertainty captured here is unlikely to cover the full range of plausible vulnerability functions. For example, it will not capture the uncertainty arising from how the function may translate to other demographics, or the fact that the function itself may take an alternative form completely. Identifying or carrying out further relevant studies in the UK would allow for a broader range to be sampled, similar to Stalhandske et al. (2022), who construct the uncertainty in their equivalent vulnerability function using six studies based on a range of employment types and regions of the world. When applying to a real world example, this selection of the form of the function and range of relevant parameters must be carefully considered, based on as much relevant information and data as possible.

3. Results and discussion

In this section we firstly demonstrate the how the risk assessment framework of Dawkins et al. (2023) (described in Section 2.1 and Fig. 1) can be used to estimate a probabilistic predictive distribution for climate risk, providing context (i.e. a baseline) for the U&SA presented subsequently. This is done based on the outdoor physical working capacity application and for one set of input factors. Following this, we present the results of the U&SA, applied to the same example, varying the inputs of the assessment as described in the previous sections to address questions 1–4 in Section 2.2.

3.1. Results: A 'baseline' climate risk assessment

The risk assessment modelling chain is applied to the set of modeler's choices highlighted in bold in Fig. 1 to provide a 'baseline' risk as context for the U&SA. For this demonstration, the 20 year time slice representative of a 2 °C above pre-industrial warming level is used from each bias corrected UKCP18 RCM ensemble member. Each hazard event is a day within this 20 years and the intensity of each hazard event at each 12 km land grid cell in the UK is characterised in terms of the Humidex heat-stress metric. This is combined with the number of people working in physical outdoor jobs, taken from SSP2 (middle of the road) in the representative 2 °C warming level year (2041), and the vulnerability function of Foster et al. (2021), based on the mean estimates of the function parameters. The end-to-end assessment, as shown in Fig. 1, produces 1000 samples of risk (here quantified as the Expected Annual Impact, EAI) spatially coherently in each UKCP18 12 km grid cell across the UK. Specifically, EAI here is the expected annual total number of days of physical outdoor work lost due to heat-stress (per year). Fig. 4 presents the resulting maps of the mean and upper and lower 95% prediction interval of risk for this application, as well as the distribution of the spatially aggregated risk based on the 1000 GAM samples. These show how, as would be expected, the risk is highest in highly populated regions of the UK (more people exposed), and

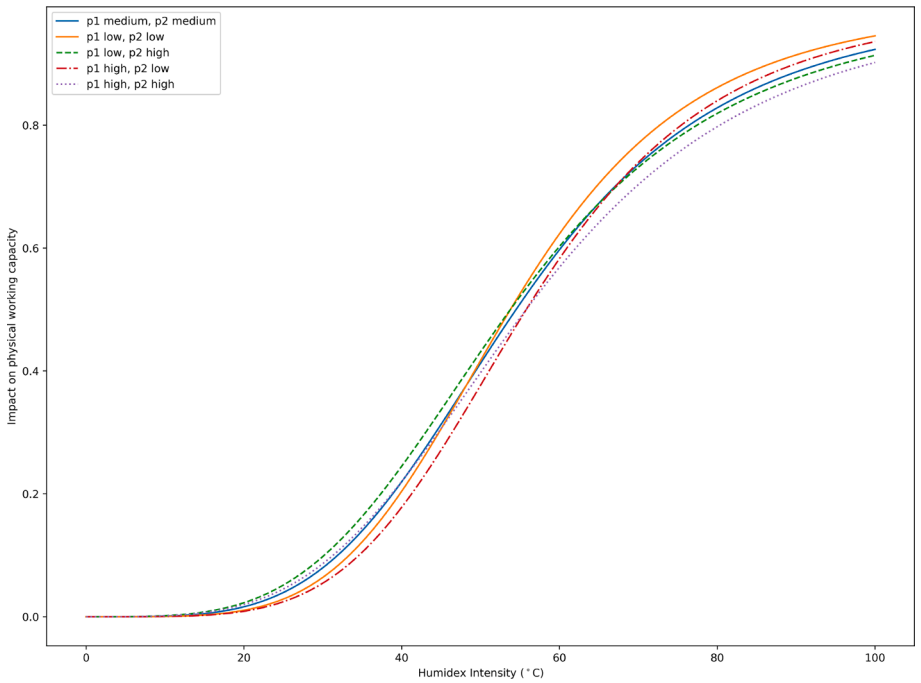

Fig. 3. A comparison of the vulnerability function when using the upper and lower bound of the confidence intervals of the two function parameters (taken from Foster et al., 2021). The function representative of the parameters means is also include.d for reference.

that the uncertainty of risk is also highest in these places.

The histogram shown in Fig. 4 (d) summarises the estimated expected number of days of physical outdoor work lost due to heat-stress in an average year at the 2 °C warming level, when aggregated over all of the UK (based on the selected input settings). For context, in this baseline example, the total number of physical working days in a year in the UK (from SSP2 for the year 2041) is 890 million (assuming all days are working days). Hence, the loss of 25 million days due to heat stress (approximately the mean of the predictive distribution in Fig. 4 (d)) equates to approximately a loss of 3% of available days. Occupational heat stress directly hampers physical work capacity, causing large economic loses for industries and regions vulnerable to global warming (Foster et al., 2021). As such, results shown in Fig. 4 (d) can also be used to estimate the subsequent expected annual financial loss for the UK by multiplying each day of work lost by an estimate of the cost this would incur. For example, suppose for demonstration that the daily loss value is £100, the mean of the distribution in Fig. 4 (d) (approximately 25 million days) equates to an expected UK total annual loss of £2.5 billion, with the upper tail of the distribution equating to a loss of approximately £3.5 billion.

3.2. Results: uncertainty analysis

In this section we explore the uncertainty in risk, based on the application described in the previous section, when applying the end-to-end framework to a range of inputs. This addresses questions 1 and 2 of Section 2.2.

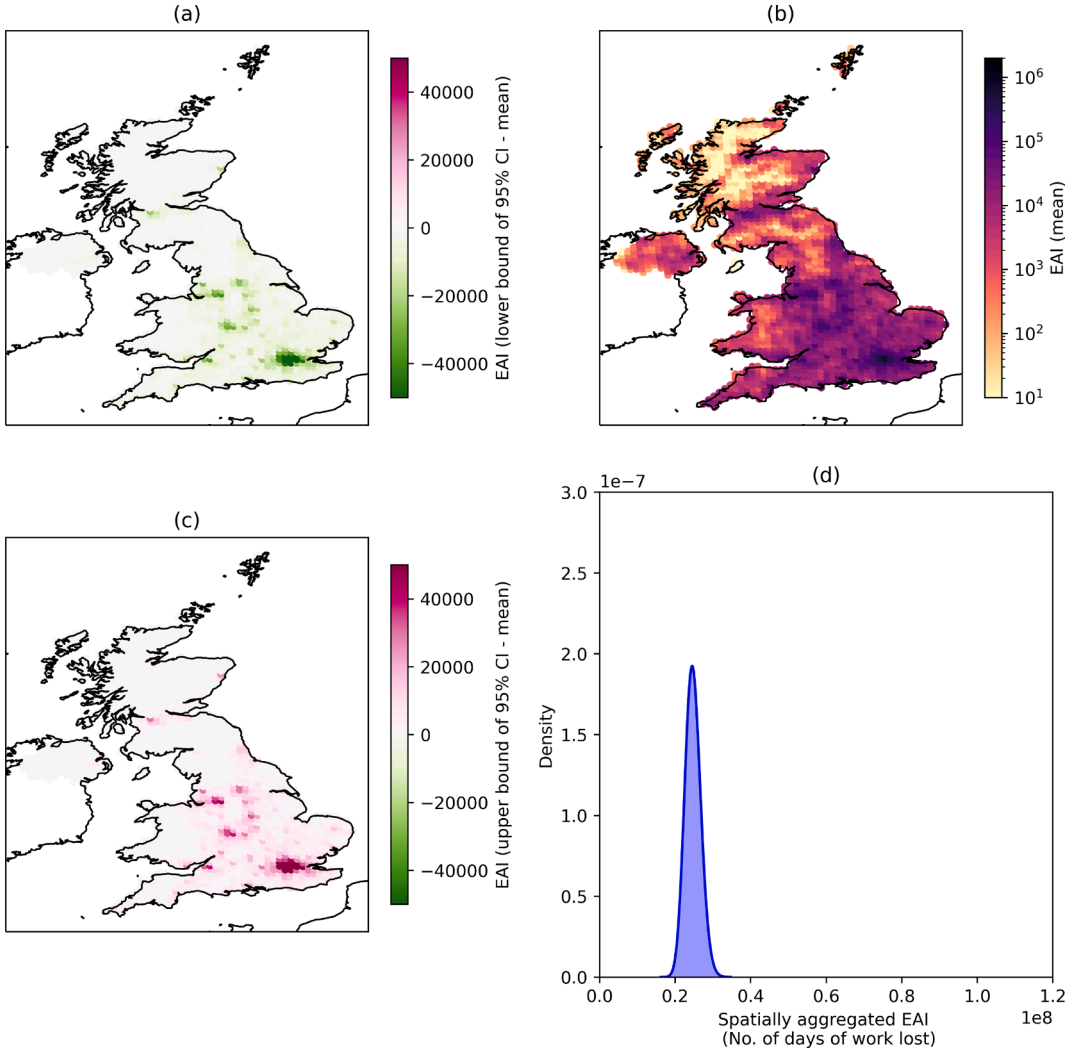

Fig. 4. Results of the 'baseline' estimation of risk (defined as the expected annual impact, EAI), and uncertainty quantification enabled by the GAM statistical modelling framework (using 1000 samples from the GAM): (a) the lower bound of the 95% prediction interval of risk (relative to mean risk); (b) the mean of the predictive distribution of risk; (c) the upper bound of the 95% prediction interval of risk (relative to mean risk); and (d) the distribution of spatially aggregated risk across the 1000 GAM samples. The x-axis range in (d) is consistent with Figs. 5 and 6 (b) to allow for direct comparison. In all plots the units of EAI is 'number of days of physical work lost due .to heat stress'.

3.2.1. Uncertainty in risk due to hazard uncertainty

Firstly, to address question (1) 'How does risk compare when estimated using different hazard data sources?', the uncertainty in risk is explored focusing on the hazard data source and calibration method inputs, keeping the exposure and vulnerability inputs fixed at SSP2 and the mean of the vulnerability parameters. The end-to-end framework (Fig. 1) is applied to all hazard data sources described in Section 2.3 and the Supplementary Material. Namely UKCP18 RCM (uncalibrated), UK-CORDEX, CMIP6 (HighResMIP), DePreSys4, and Observations, as well as data produced using the two calibration approaches: bias correction, and change factor (see Section 2.4), both applied to the UKCP18 RCM data using historical observations as the 'truth'. The calibration approaches are not applied to other datasets due to time limitations of the study. The resulting 1000 GAM samples of risk are then each aggregated over space and the distribution of spatially aggregated EAI compared, as shown in Fig. 5.

Fig. 5 (a) shows how all uncalibrated data sources underestimate risk in the recent historical period. Additional validation of the hazard data (not shown) identified that this is due to a spatially consistent underestimation of daily maximum temperature. Of the uncalibrated data sources, UKCP18 (raw) shows best agreement with the observed spatially aggregated EAI calculated empirically for the same period (black line). However, agreement is greatly improved when the bias corrected equivalent is used. The DePreSys hindcast data is the only data source where the distribution of spatially aggregated EAI does not overlap the observed value, and this distribution is less wide then other uncalibrated sources. This difference is not yet fully understood and further validation and research is needed here. It is hypothesised that this may be due to the reinitialisation of the hindcasts (see Supplementary Material), meaning that the ensemble members are likely to behave more similarly than the free running climate projection simulations. Further, as shown in Table 1, the two data sources that are most biased compared to observations are those with the lowest spatial resolution (DePreSys: 60 km and CMIP6: ~50 km). This potentially suggests that resolution may also plays a role in how well a data source is able to represent hazards and therefore risk. It should be noted, however, that differences in the models and model set ups haven't been controlled for

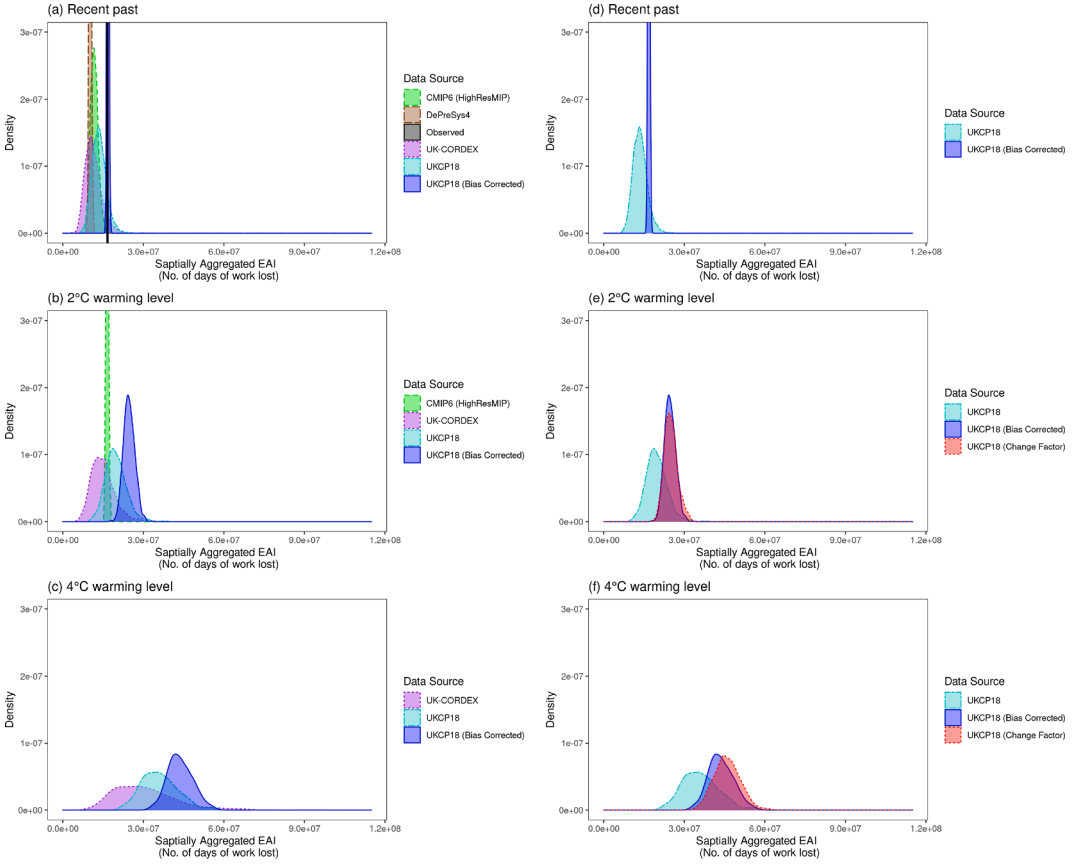

Fig. 5. Results of the uncertainty analysis addressing question (1) 'How does risk compare when estimated using different hazard data sources?' Each panel shows the predictive distribution of spatially aggregated risk (expected annual impact, EAI) under different hazard data sources. The left column compares different climate models (including bias corrected UKCP18 for comparison), and the right column compares different calibration approaches (including uncalibrated UKCP18 for comparison). The top row (a and d) shows this for the recent historical period (1998–2017), the middle row (b and e) for the 2 °C warming level, and the bottom row (c and f) for the 4 °C warming level. Some data sources do not appear in all rows (e.g. CMIP6 is not presented in c) due to the lack of data at that warming level (as described in Section 2.5). Note that the predictive distribution in panel (b) with bias corrected UKCP18 data is the same as in Fig. 4 (d), and that the x-axis ranges are consistent with Figs. 4 (d) and 6 (b) to allow for di.rect comparison.

here, hence this cannot necessarily be associated with model resolution only.

The equivalent distributions of risk in the future warming levels (Fig. 5 (b) and (c)) show how, for all hazard data sources, risk is expected to increase, with the uncertainty becoming greater as ensemble members diverge (as is often seen in climate projection plots Lowe et al., 2018). The CMIP6 (HighResMIP) distribution becomes less wide in Fig. 5 (b) because less ensemble members are included due to data availability (noting that only 4 CMIP6 HighResMIP ensemble members are included in this analysis limiting data availability, see Table 1 in the Supplementary Material). In these future warming level plots, it can be seen that the uncalibrated data sources continue to underestimate risk compared to the bias corrected data, most notably for UK-CORDEX for the 4 °C warming level. This highlights the importance of calibrating climate data, particularly when using it to calculate absolute risk (as opposed to changes in risk between time periods).

Fig. 5 (d) - (f) shows the equivalent uncertainty in spatially aggregated EAI comparing the two calibration approaches applied to the UKCP18 RCM data. These plots show how, although there is general agreement between the spatially aggregated risk predictive distributions in Figs. 5 (e) and (f), there are some subtle differences. In particular, the change factor approach gives overall slightly higher risk estimates at the 4 °C warming level.

Due to the underestimation of risk in the uncalibrated climate datasets (Fig. 5 a), and as calibration of all data sources was beyond the scope of this study, these data sources (UK-CORDEX, CMIP6 HighResMIP, DePreSys4) are discarded for the remainder of the analysis, and the hazard data source input is fixed as UKCP18. Future work should aim to apply the calibration approaches to the other hazard data sources to facilitate their usage in climate risk assessments and sensitivity studies.

3.2.2. Uncertainty in risk due to hazard, vulnerability and exposure uncertainty

To address question (2) 'How uncertain is risk when considering all plausible inputs (that is, when varying not only hazard source but also exposure and vulnerability)?', Fig. 6 presents the uncertainty in risk when applying the end-to-end framework to the exhaustive sample of all input settings (see Fig. 1):

- Hazard: data source fixed at UKCP18 but with different calibration methods (i.e. no calibration, bias correction, change factor);
- Warming level: global mean temperature 2 °C above pre-industrial, global mean temperature 4 °C above pre-industrial;
- SSP: UK SSP1 (sustainability), UK SSP2 (middle of the road), UK SSP5 (fossil fuelled development);
- Vulnerability function parameter 1: lower bound, mean value, upper bound;
- Vulnerability function parameter 2: lower bound, mean value, upper bound;

Fig. 6 (a) shows how, consistent with Fig. 4, the uncertainty in risk across all the varied inputs is highest in highly populated regions where exposure is high. In particular, there is a large uncertainty in regions of Scotland where SSP5 leads to high urbanisation. Fig. 6 (b) highlights the increased uncertainty in risk when the inputs are varied, compared to when considering only one set of inputs (as in Fig. 4 b). The upper tail of the distribution of risk is now approximately 110 million days (equivalent to 12% of potential days), much larger than the range in Fig. 4 (d). This highlights how under-representing the plausible range of risk could have an important impact on the consideration of plausible extremes relevant for adaptation decision making, and hence the importance of exploring these uncertainties. Specifically, exploration of the data identifies that the most extreme risk outcomes are associated with a combination of

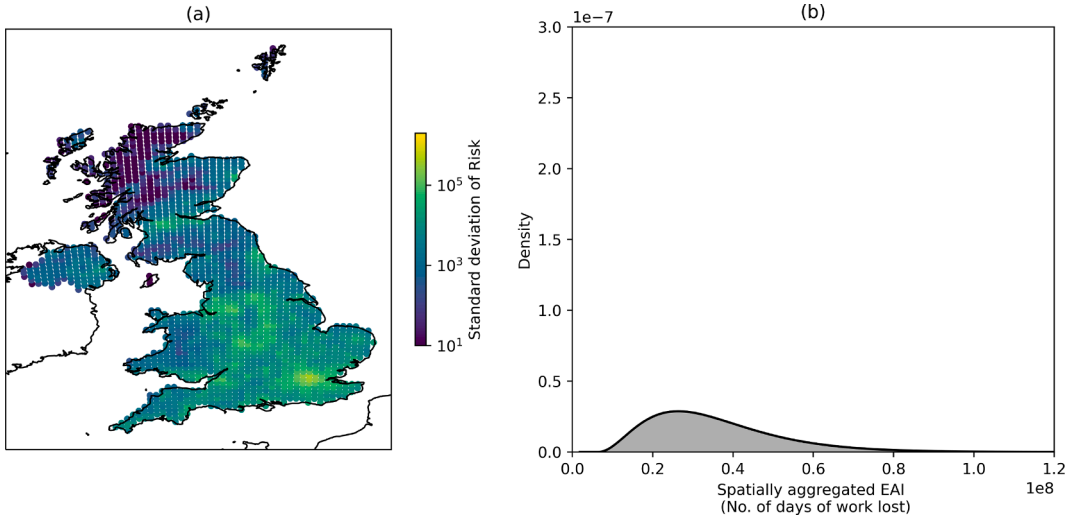

Fig. 6. Results of the uncertainty analysis addressing question (2) 'How uncertain is risk when varying all plausible inputs (hazard, exposure and vulnerability)?': (a) the standard deviation of risk (EAI) at each location, calculated based on all GAM samples produced by varying all input settings (but the hazard data source, which is fixed to UKCP18); (b) the associated distribution of spatially aggregated risk across all the same input settings. The x- and y-axis ranges in (b) are consistent with Figs. 4 (d) and 5 to allow for di.rect comparison.

three input factors: 4 °C warming level, SSP5 and the upper bound of parameter 2 of the vulnerability function.

3.3. Results: sensitivity analysis

In this section we explore the sensitivity of risk, based on the same application. This addresses questions 3 and 4 of Section 2.2.

3.3.1. Sensitivity of risk to hazard, vulnerability and exposure uncertainty

Initially, the PAWN sensitivity analysis methodology is applied to the exhaustive global sample of all combinations of input factors (listed in the previous section). As described in Section 2.2, the sensitivity analysis approach requires a 1–2-1 mapping between the inputs and output. Therefore, in each plot we specify a specific summary statistic of the predictive distribution of risk as the output. Fig. 7 helps to graphically visualise how sensitive the output is to varying each input. Here the output is the mean of the predictive distribution of spatially aggregated EAI (i.e. the mean of the distributions shown in Fig. 5). Fig. 7 (b), for example, shows that there is a large difference between the unconditional and conditional output CDFs when the warming level input is varied. Further, as may be expected, the output risk is higher for the higher warming level (i.e. the CDF is lower for any given value of the output). Similarly, Fig. 7 (c) shows how SSP5 results in much higher output risk, compared to the other two SSPs.

In addition, the uncalibrated UKCP18 dataset has a CDF separated from the others in Fig. 7 (a), representing lower output risk values (consistent with Fig. 5). This further shows the underestimation of risk when using uncalibrated data, again highlighting the need to calibrate climate data when exploring absolute risk values. The calibrated data sources are largely consistent indicating that, in this example, the output used here (predicted mean risk) is relatively insensitive to the approach used for calibration.

The results in Fig. 7 also show how lower values of vulnerability function parameter 1 and higher values of vulnerability function parameter 2 lead to higher risk, this is consistent with the orange curve in Fig. 2 which results in the highest impact when Humidex is less than approximately 50 °C (as is predominantly the case in the UK). Moreover, differences in the conditional CDF for parameter 2 are larger than parameter 1, showing that the sensitivity of the output risk is greater for parameter 2 (the steepness of the vulnerability curve). The sensitivity of the output to each input is summarised by the sensitivity indices shown in Fig. 8. Again, following the PAWN method, each sensitivity index is calculated as the mean Kolmogorov–Smirnov (KS) statistic between the unconditional and the conditional CDFs of the output. This analysis is repeated for three possible definition of the output: (a) the *mean* of the distribution of

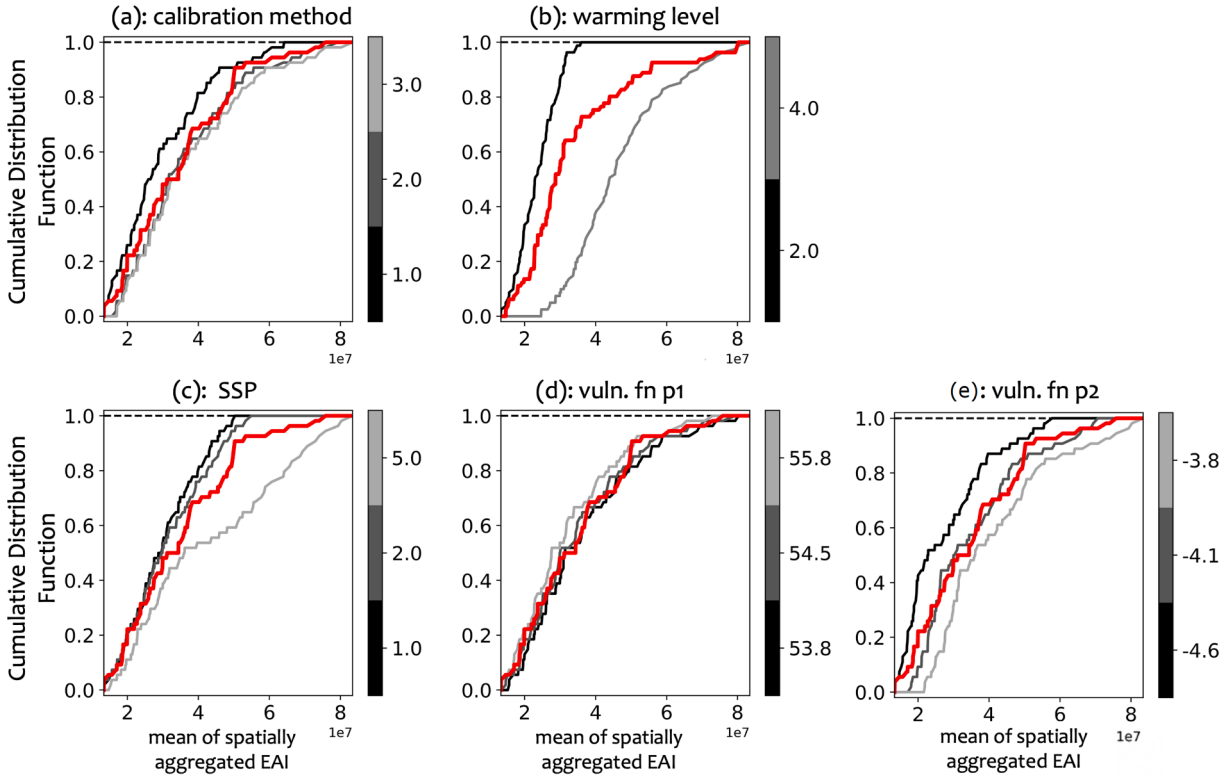

Fig. 7. Cumulative Distribution Functions (CDFs) of the output risk metric (defined as the mean of the predictive distribution of spatially aggregated EAI) when varying all the inputs (red), and when varying all inputs but one, which is held fixed at each of its possible values (conditional CDFs in grey). Each plot shows a different conditioning input: (a) Calibration method (possible choices: 1 = UKCP18 uncalibrated, 2 = UKCP18 bias corrected, 3 = UKCP18 Change Factor); (b) Warming level (2 °C and 4 °C); (c) SSP (1, 2 and 5); (d) Vulnerability function parameter 1 (lower bound = 53.8, mean = 54.5, upper bound = 55.8); and (e) Vulnerability function parameter 2 (lower bound=-4.6, mean=-4.1 and upper bound=-3.8).

spatially aggregated risk (i.e. the sensitivity indices are the KS statistics between the CDFs shown in Fig. 7)); and the *lower* (b) and *upper* (c) bounds of the 95% prediction interval of the risk distribution, which capture a measure of the uncertainty in risk (see also Fig. 1).

Addressing question 3 from Section 2.2 'What is the relative sensitivity of risk to the components of the risk modelling chain (i.e. hazard, exposure and vulnerability)?', Fig. 8 (a) shows how the mean spatially aggregated risk is most sensitive to variations in the warming level, followed by parameter 2 of the vulnerability function, with the other three inputs leading to similar sensitivity. This is consistent with Fig. 7. The high sensitivity to the warming level may be expected given it is a very large source of uncertainty. The relatively high sensitivity to the vulnerability function parameter (p2) is more surprising considering the relatively small amount this parameter is varied in this study (see Fig. 2). This is a good demonstration of how sensitivity analysis is able to identify inputs that disproportionately affect outputs. This then highlights the further need to explore how varying this function more broadly (e.g. in space, time and demography) affects the output risk. Similarly, it should be noted that the relatively low sensitivity to the vulnerability function parameter p1 may result from the small uncertainty range sampled (see Fig. 3), and this outcome may differ if a broader range is considered. It is interesting to note the relatively low sensitivity to SSP (when considering the UK as a whole). Referring back to Fig. 7, this is likely due to the similarity between SSP1 and SSP2 in the exposure metric considered within this study (number of people in outdoor physical jobs).

Similar results are shown for the upper and lower bounds of the 95% prediction interval of the predictive distribution of spatially aggregated risk (Fig. 8 b and c). However, the sensitivity to calibration method is slightly higher for the lower bound (and lower for the upper bound). This is consistent with the results shown in Fig. 5 (e) and (f), where the calibrated and uncalibrated distributions are most different in the lower tail. This suggest that calibrating the hazard data is important, particularly to ensure the lower tail of the risk distribution is not underestimated, as this may have implications for adaptation decision making. In most cases the sensitivity indices are above the threshold of statistical significance (dashed line), meaning that risk is significantly sensitive to all inputs to some degree. An equivalent sub-analysis for exploring the sensitivity of risk to the timing of the warming levels (i.e. the year used from the SSP data to represent each warming level) is presented in Fig. 1 of the Supplementary Material. As described in Section 2.6, this analysis uses SSP5 only, but varies the years used to represent the 2 °C and 4 °C warming levels. This is done separately from the main analysis to avoid highly implausible SSP:warming level combinations. This indicates that risk is relatively insensitive to varying the

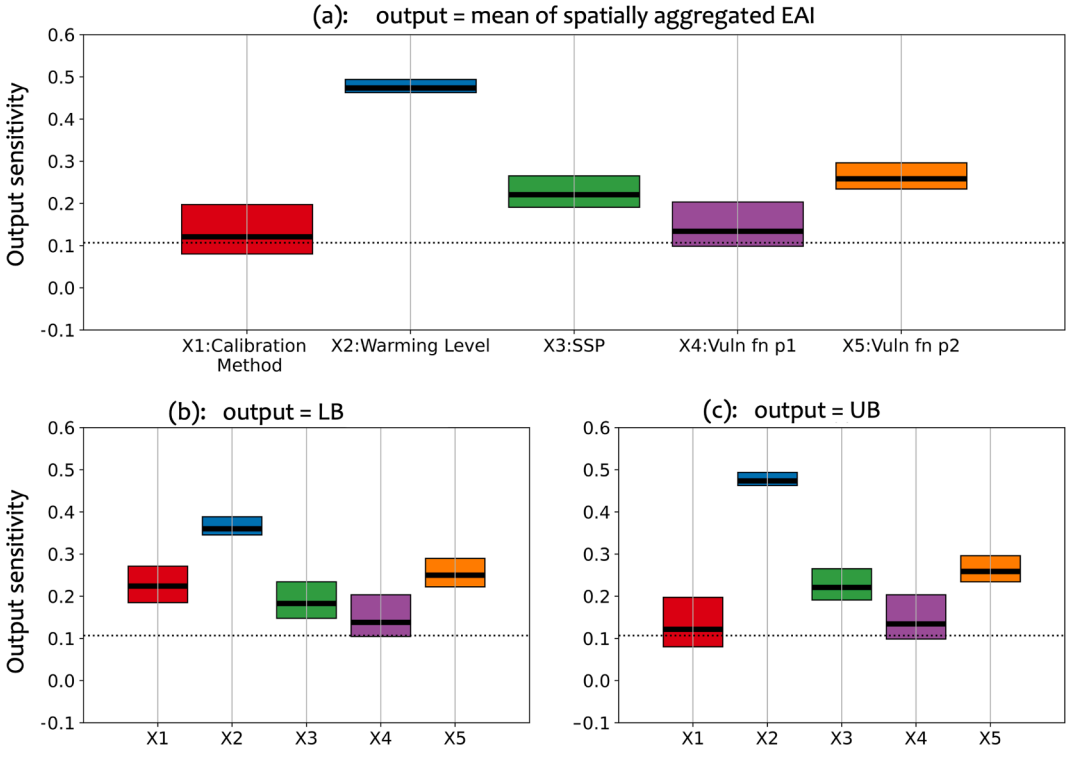

Fig. 8. Results of the sensitivity analysis addressing question (3) 'What is the relative sensitivity of risk to the components of the risk modelling chain (i.e. hazard, exposure and vulnerability)?': sensitivity indices (mean Kolmogorov–Smirnov statistic between the unconditional and the conditional CDFs of the output) for three definitions of the output metric: (a) the mean of the predictive distribution of spatially aggregated EAI; (b) the lower bound (LB) of the 95% prediction interval of spatially aggregated EAI (i.e. the 5% quantile of the predictive distribution sampled from the GAM); and (c) the equivalent upper bound (UB). The box captures the spread in the sensitivity indices when calculated based on 5000 bootstrap samples of the inputs and output, with the mean of this bootstrap sample indicated by the solid black line within the box. A higher value of the sensitivity index means that the output is more sensitive to the corresponding input. The horizontal dashed line indicates the critical value below which no significant sensitivity can be detected (calculated as the critical value for the test of statistical significance of the KS statistic at the 95% level (.Smirnov, 1948)).

timing of the warming level, with the box-plot of the sensitivity index intersecting with the statistical significance threshold for all output metrics.

3.3.2. Sensitivity of risk across the spatial domain

In order to answer question 4 from Section 2.2 'How does this sensitivity vary in space, across the UK region?', the PAWN analysis is repeated for each location separately (using the original set of input factors, varying SSP rather than SSP year). The resulting spatial maps of the sensitivity indices for the mean of the predictive distribution of risk are shown in Fig. 9. These show the same general results as discussed in relation to Fig. 8, but now allow for the spatial variability in the sensitivity to be explored. For example, Fig. 9 (b) shows that risk is generally more sensitive to warming level in the south of the UK, compared to the north, consistent with UKCP18 findings (see Fig. 2.6 in Lowe et al., 2018). Further, Fig. 9 (c) highlight regions in which risk is more sensitive to SSP, in particular urban areas and parts of Scotland. This is due to the increased urbanisation, particularly in Scotland, seen in future years of SSP5.

These results highlight how different regions of the UK could benefit from different areas of future research focus. In addition, while there are many other factors that go into adaptation decision making (including cost, local acceptance and context specific side effects), these results can help to describe the potential for different targeted forms of adaptation in reducing risk. For example, in the regions where risk is most sensitive to the SSP, future research should look to refine and better understand the plausibility of the future population projections, and adaptation could include socio-economic measures to minimise the likelihood of SSPs that lead to high risk (i.e. SSP5). Conversely, in regions most sensitive to warming level, focus on mitigating the warming of the climate may seen to be of more importance.

4. Limitations

As widely discussed in the sensitivity analysis literature, the conclusions of any U&SA depend on the definition of the space of variability of the inputs (Pianosi et al., 2016; Kropf et al., 2022). As a result, while this study goes some way in exploring the uncertainties and sensitivities of climate risk in the application presented, there are many more input settings that could be explored. For example, only three SSPs, only a set of climate data sources and calibration approaches, and only a limited representation of the vulnerability function is used. A more extensive study including more input choices could have provided different conclusions to those shown here. Further, when using such an approach to explore stakeholder risk and the associated uncertainties and sensitivities, it is important to select input settings that are of key relevance to the decision making processes of that stakeholder. This may involve working with the stakeholders to understand their exposures (i.e. asset distribution), vulnerabilities, risk tolerance and the costs and benefits of different decisions or actions, which may require substantial time commitments. While the importance of U&SA has been

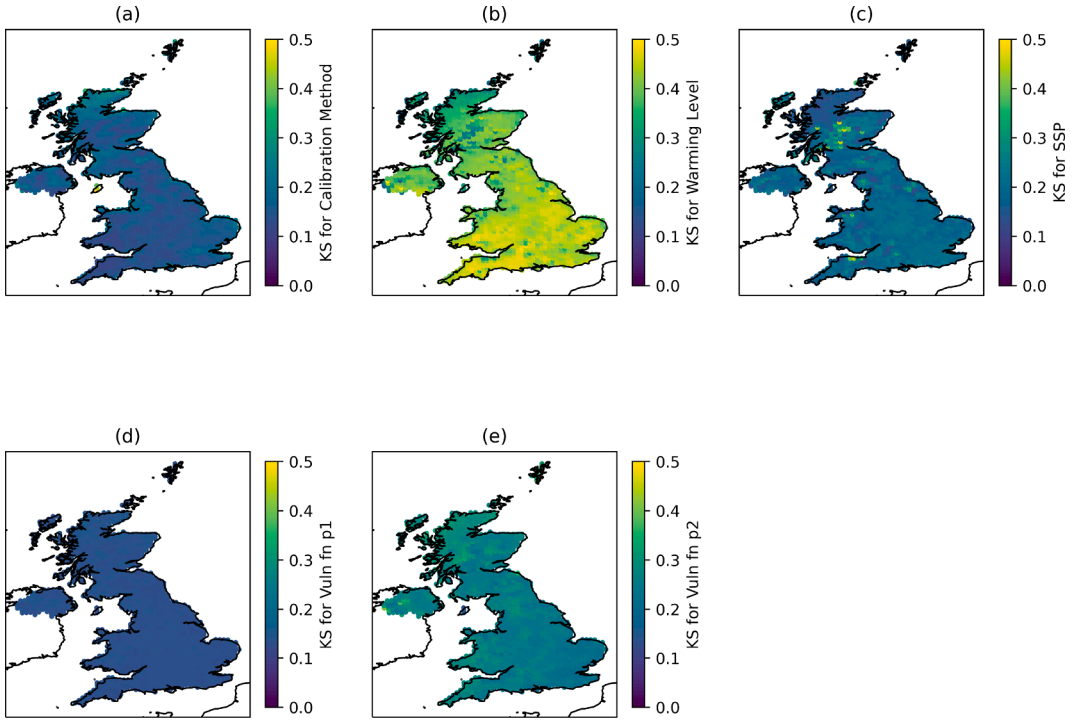

Fig. 9. Results of the sensitivity analysis addressing question (4) 'How does risk sensitivity vary in space, across the UK region': sensitivity indices in each grid cell (mean of 5000 bootstrap samples) for each input factor (a: Calibration method, b: Warming level, c: SSP, d: Vulnerability function parameter 1, e: Vulnerability function parameter 2). The output risk metric is the mean of the predictive distribution of EAI in each location.

demonstrated here and has been well known within the research community for a long time, it is not standard practice in real-world applications, likely due in part to the complexity of carrying out a realistic and meaningful analysis. Engagement with potential users has highlighted that, in many cases, the exposure, vulnerability and adaptation decision information and understanding required for a useful and usable climate risk assessment and U&SA is unavailable, and that the within user-organisation expertise in this area is often limited. As a result, there is a strong need for climate/risk modellers to work in closer partnership with organisations to both help develop a common understanding of the information and data required to make better decisions, and to help develop the expertise needed for adopting approaches such as those presented in this study.

Similar to Dawkins et al. (2023), in the application used in this study the vulnerability function is the same across the spatial domain and regardless of demographics. In a more real-world application it would be important to more realistically represent different people/assets/ecosystems using different vulnerability functions. Further, it must be ensured that the vulnerability function is able to relate external hazard conditions (e.g. temperature) with the risk, which in many cases may be related to indoor conditions. As noted by Dawkins et al. (2023), this will likely require the exploration of data from physical building stock model analysis, such as Grassie et al. (2022), or weather sensor data.

Throughout, the results presented within this study focus predominantly on means, e.g. defining risk as the expected annual impact, and predominantly using the mean of the predictive distribution of risk in the PAWN sensitivity analysis. Future work should look to explore alternative summary metrics, determined to be of most relevance to the user and their decision making. As discussed in Dawkins et al. (2023), a risk metric such as the 1 in 10-year event may be more relevant for adaptation decision making, when a stakeholder is concerned with extreme 'shock' events. In this case, the analysis steps in Fig. 1 would be carried out using this alternative risk metric, derived from the risk assessment. In this labour productivity application, the ensemble mean 1 in 10-year event for the 2 °C warming level results in approximately 30% of potential outdoor physical work being lost.

Further, this study only explores the translation of hazard to risk, and not how risk estimates inform decisions for climate adaptation. Future research should explore how this framework could be further developed to become an adaptation decision support tool, and U&SA used to investigate how hazard, exposure and vulnerability uncertainties control not only risk quantification but also adaptation decisions. Kropf et al. (2022) present an U&SA of adaptation options for a case in Vietnam using the CLIMADA unsequa module, motivated by the conclusions of Bresch and Aznar-Sigua (2021), hence an equivalent extension of the framework developed here could be pursued to compliment this work.

5. Implications for risk management

Most significantly, this study has shown how varying the inputs and approaches used in a climate risk assessment can lead to a very different quantification of risk. This highlights the need to explore such uncertainties and sensitivities when carrying out a climate risk assessment, and shows that important adaptation and/or policy decisions should not be based on just one (or a small number of) plausible inputs (e.g. using only the Chartered Institution of Building Services Engineers (CIBSE) weather files (Mylona, 2012)). In particular, this study has shown how uncertainty analysis can help to identify plausible extremes resulting from particular combinations of input factors; and how sensitivity analysis can help to identify key areas of future research focus and possible key adaptation approaches. While a thorough U&SA may take more time and effort, it will provide a greater wealth of information upon which to make decisions, help to identify key areas that require a better understanding, and ultimately help to highlight where decision making is most robust (i.e., invariant to changing the input factors), leading to greater confidence in the action taken. As discussed in Section 4, while the analysis presented here explores a number of sources of uncertainty, many more could be included, specifically those that might be important for a given user. As such, the results of this study should be considered as evidence that U&SA is a key part of the risk management process, and as a demonstration of an approach for carrying out U&SA. This approach would, however, likely need to include additional relevant factors if applied to specific stakeholder adaptation decision making and planning. In this illustrative case for example, the economic cost of days of labour lost and a more nuanced view of the changes in demand for physical labour in different sectors owing to increased mechanisation etc.

In addition, the results of the study demonstrated the importance of calibrating climate model data, particularly when it is being used to represent absolute values, rather than changes between time periods, as was the case here. In the application presented, the approach for calibration was generally shown to be less important than other input factors, however this may not be the case for a different hazard, risk metric or region, and should therefore still be explored in each case.

One important aspect to consider is the implication of the sensitivity analysis for the construction and use of high impact low likelihood (HILL) scenarios or reasonable worse case scenarios, which are relevant for stress testing in a number of sectors including finance and infrastructure design. In particular, the current study provides a guide for the elements that need to be considered in a HILL scenario and especially point towards including elements beyond hazard. For instance Fig. 8 suggests elements of vulnerability and exposure should both also be considered in constructing a HILL scenario for heat related labour issues.

6. Conclusion

This study has presented a demonstration of an approach for extending the CLIMADA based risk assessment framework of Dawkins et al. (2023) to explore the uncertainty and sensitivity of climate risk when simultaneously varying inputs in the hazard, exposure and vulnerability components. Here, rather than specifying a probability distribution for each input factor (as in Kropf et al., 2022), we define a discrete set of choices considered to be plausible by the scientific community, for example using exposure information from a selection of future population projections (SSPs) and using hazard information from a selection of climate data products (e.g. UKCP18,

CMIP6 and UK-CORDEX). We do this because, in practice it is often very challenging to meaningfully define all input uncertainties using probability distributions. Using a discrete set of inputs also has the advantage that we can directly relate our output back to the specific inputs combination used to generate it.

We demonstrate the application of this method, focusing on the risk of reduced outdoor physical working capacity in the UK as a result of extreme heat and humidity. Specifically, climate risk is represented by the expected number of days of physical outdoor work lost in a given year due to heat-stress. This risk metric is calculated based on input factors representing the hazard data source, the calibration method, the global warming level, the SSP (where the year from the SSP projection used to represent the warming level must be specified), and the two parameters of the vulnerability function. Based on these input factor settings, we demonstrate an approach for answering two Uncertainty Analysis questions: (1) How does risk compare when estimated using different hazard data sources? (2) How uncertain is risk when considering all plausible inputs? And two Sensitivity Analysis questions: (3) What is the relative sensitivity of risk to the components of the risk modelling chain (i.e. hazard, exposure and vulnerability)? (4) How does this sensitivity vary in space, across the UK region?.

Related to question (1), we show that all uncalibrated data sources underestimate risk in the recent historical period, highlighting the importance of calibrating/bias-adjusting climate data when quantifying absolute risk. Further, we show how the two calibration approaches (bias correction and change factors) show generally good agreement but that the change factor approach gives overall slightly higher risk estimates at the higher, 4 °C warming level.

Related to question (2), we show how the full predictive distribution of spatially aggregated risk gives a much greater range of plausible outcomes than if only considering hazard uncertainty, highlighting the importance of considering all sources of uncertainty simultaneously. In particular, we identify the most extreme outcomes to be produced by the 4 °C warming level under the SSP5 scenario and with the upper bound of parameter 2 of the vulnerability function (the steepness of the function).

Related to question (3), we find that, in our application, the predictive distribution of spatially aggregated risk is most sensitive to variations in the warming level (highlighting the importance of meeting the climate change policy goals set out by the Paris Agreement which align with a 2 °C warming by 2100 (Betts and Brown, 2021)), followed by variations in one of the two parameters of the vulnerability function. The relatively high sensitivity to the vulnerability function parameter is somewhat surprising given the relatively small amount these parameters are varied in this study, providing a good demonstration of how sensitivity analysis is able to identify inputs that disproportionately affect outputs. An additional analysis is carried out to quantify the sensitivity of risk to the year within the SSP record used to represent each warming level, indicating relatively low sensitivity to this factor.

Related to question (4), we show that risk is generally more sensitive to warming level in the south of the UK, compared to the north, and identify key regions where risk is instead most sensitive to SSP, regions in which SSP5 leads to large urbanisation. This shows how different regions of the UK could benefit from different areas of research focus and different targeted forms of adaptation. Namely how those areas most sensitive to SSP may benefit most from socio-economic measures to minimise the likelihood of population evolution similar to SSP5, and how those areas more sensitive to the vulnerability function may benefit most from research to better define this function.

Future work should explore the development of an adaptation decision tool as an extension of the framework. Similar to Bresch and Aznar-Sigua (2021) and Kropf et al. (2022), this would allow for the quantification of the cost and benefit of different possible adaptation measures, and hence the exploration of plausible optimal pathways to improved resilience. Rather than focusing solely on the financial benefit, this tool could be based on multiple factors by employing a multi-attribute Bayesian decision analysis framework (Smith, 2010; Dawkins et al., 2021). This takes uncertain information about the 'state of nature' (i.e. risk) and combines it with information about possible adaptation options and the preferences of the decision maker, to identify the adaptation option that maximises the expected utility/pay-off. This could be applied to each location/asset to provide a spatially coherence picture of optimal adaptations across a region (e.g. the UK). In doing so, a number of other uncertain inputs are introduced into the modelling processes. Expert elicitation with the user/decision maker could help to identify a range of plausible values for these inputs which could be included within an U&SA, highlighting when and where decision making is sensitive to particular input factors or assumptions. While this may be challenging to achieve in a real-world application, this would ultimately provide spatially coherent maps of 'optimal' adaptation actions (based on the assumptions of the inputs used), as well as a demonstration of the sensitivity of this outcome to varying the uncertain inputs. This would be valuable insight that could contribute towards the next UK Climate Risk Assessment (CCRA4). As such, as discussed in Dawkins et al. (2023), an important next step is to explore the application of this framework to a user-specific real-world example, to understand it's potential to inform stakeholder climate risk and adaptation decision making.

Data statement

The data used and code developed within this study are available upon request.

Author contributions statement

L.D.: Conceptualization, Methodology, Software, Validation, Formal Analysis, Writing, Visualization.
D.B.: Conceptualization, Supervision.
F.P.: Guidance, Writing, Visualization.
T.E.: Guidance.
J.L.: Guidance.

Declaration of Competing Interest

The authors declare that they have no known competing financial interests or personal relationships that could have appeared to influence the work reported in this paper.

Data availability

Data will be made available on request.

Acknowledgements

This work (and the time of L.D., D.B. and J. L.) was funded under the Strategic Priority Fund for UK Climate Resilience. The UK Climate Resilience programme is supported by the UKRI Strategic Priorities Fund. The programme is co-delivered by the Met Office and NERC on behalf of UKRI partners AHRC, EPSRC and ESRC. T.E. was funded by the European Union's Horizon 2020 research and innovation programme under grant agreement No. 856612 https://ec.europa.eu/info/research-and-innovation/funding/funding-opportunities/funding-programmes-and-open-calls/horizon-europe_en and the Cyprus Government. J. L. and F. P. are partially supported by the UK Natural Environment Research Council through a Climate and Environmental Risk Analytics for Resilient Finance (CERAF) grant [NE/V017756/1].

Appendix A. Supplementary material

Supplementary data associated with this article can be found, in the online version, at https://doi.org/10.1016/j.crm.2023.100511.

References

Arnell, N.W., Freeman, A., Kay, A.L., Rudd, A.C., Lowe, J.A., 2021. Indicators of climate risk in the uk at different levels of warming. Environ. Res. Commun. 3 (9), 095005.
Aznar-Siguan, G., Bresch, D.N., 2019. CLIMADA v1: a global weather and climate risk assessment platform. Geosci. Model Develop. 12, 3085–3097.
Barnes, C.R., Chandler, R., Brierley, C., 2022. Comparison of EuroCORDEX output with UKCP18 regional ensemble. Technical report.
Betts, R.A., Brown, K., 2021. Introduction. In: The Third UK ClimateChange Risk Assessment. Technical report.
Bresch, D.N., Aznar-Sigua, G., 2021. CLIMADA v1.4.1: towards a globally consistent adaptation options appraisal tool. Geosci. Model Dev. 14, 351–363.
Cannon, A.J., Sobie, S.R., Murdock, T.Q., 2015. Bias correction of gcm precipitation by quantile mapping: How well do methods preserve changes in quantiles and extremes? J. Clim. 28, 6938–6959.
Dawkins, L.C., Bernie, D.J., Lowe, J.A., Economou, T., 2023. Assessing climate risk using ensembles: A novel framework for applying and extending open-source climate risk assessment platforms. Clim. Risk Manage., (accepted).
Dawkins, L.C., Williamson, D.B., Mengersen, K.L., Morawska, L., Jayaratne, R., Shaddick, G., 2021. Where is the clean air? a bayesian decision framework for personalised cyclist route selection using R-INLA. Bayesian Anal. 16, 61–91.
Dessai, S., Hulme, M., 2007. Assessing the robustness of adaptation decisions to climate change uncertainties: A case study on water resources management in the East of England. Global Environ. Change 17 (1), 59–72.
Ehret, U., Zehe, E., Wulfmeyer, V., Warrach-Sagi, K., Liebert, J., 2012. Hess opinions should we apply bias correction to global and regional climate model data? Hydrol. Earth Syst. Sci. 16, 2291–3404.
F., S.C., Lissner T, K., M., F.E., et al., 2016. Differential climate impacts for policy-relevant limits to global warming: the case of 1.5C and 2C. Earth Syst Dyn, 7(2): 327–351.
Foster, J., Smallcombe, J.W., Hodder, S., Jay, O., Flouris, A.D., Nybo, L., Havenith, G., 2021. An advanced empirical model for quantifying the impact of heat and climate change on human physical work capacity. Int. J. Biometeorol. 65, 1215–1229.
Garry, F.K., Bernie, D.J., Davie, J.C.S., Pope, E.C.D., 2021. Future climate risk to uk agriculture from compound events. Clim. Risk Manage. 32, 100282.
Gettelman, A., Bresch, D.N., Chen, C.C., Truesdale, J.E., Bacmeister, J.T., 2018. Projections of future tropical cyclone damage with a high-resolution global climate model. Clim. Change 146, 575–585.
Grassie, D., Schwartz, Y., Symonds, P., Korolija, I., Mavrogianni, A., Mumovic, D., 2022. Energy retrofit and passive cooling: overheating and air quality in primary schools. Build. Cities 3 (1), 204–225.
Haarsma, R.J., et al., 2016. High Resolution Model Intercomparison Project (HighResMIP v1.0) for CMIP6. Geosci. Model Dev. 9, 4185–4208.
Hanlon, H.M., abd G. Carigi, D.B., Lowe, J.A., 2021. Future changes to high impact weather in the UK. Clim. Change 116, 50.
Harmackova, Z., Pedde, S., Bullock, J.M., et al., 2022. Improving regional applicability of the UK shared socioeconomic pathways through iterative participatory co-design. Clim. Risk Manage. 37 (100452).
Herman, J., Usher, W., 2017. Salib: An open-source python library for sensitivity analysis. J. Open Source Software 2 (9), 97.
Hersbach, H., et al., 2020. The ERA5 global reanalysis. Q.J.R. Meteorol. Soc. 146 (730).
Ho, C.K., Stephenson, D.B., Collins, M., Ferro, C.A.T., Brown, S.J., 2012. Calibration strategies: A source of additional uncertainty in climate change projections. Bull. Am. Meteorol. Soc. 93, 21–26.
Hollis, D., McCarthy, M., Kendon, M., Legg, T., Simpson, I., 2019. HadUK-Grid: A new UK dataset of gridded climate observations. Geosci. Data J. 6, 151–159.
IPCC (2021). Climate Change 2021: The Physical Science Basis. Contribution of Working Group I to the Sixth Assessment Report of the Intergovernmental Panel on Climate Change[Masson-Delmotte, V., P. Zhai, A. Pirani, S.L. Connors, C.Péan, S. Berger, N. Caud, Y. Chen, L. Goldfarb, M.I. Gomis, M. Huang, K. Leitzell, E. Lonnoy, J.B.R. Matthews, T.K. Maycock, T. Waterfield, O. Yelekçi, R. Yu, and B. Zhou (eds.)]. Technical report.
IPCC (2022). Climate Change 2022: Impacts, Adaptation, and Vulnerability. Contribution of Working Group II to the Sixth Assessment Report of the Intergovernmental Panel on Climate Change [H.-O. Pörtner, D.C. Roberts, M. Tignor, E.S. Poloczanska, K. Mintenbeck, A. Alegría, M. Craig, S. Langsdorf, S. Löschke, V. Möller, A. Okem, B. Rama (eds.)]. Technical report.
Iturbide, M. et al., 2021. Repository supporting the implementation of fair principles in the ipcc-wg1 atlas. zenodo. https://github.com/IPCC-WG1/Atlas. Accessed: 2022-05-25.

Jacob, D., Petersen, J., Eggert, B., Alias, A., Christensen, O.B., Bouwer, L.M., Braun, A., Colette, A., Déqué, M., Georgievski, G., et al., 2014. EURO-CORDEX: new high-resolution climate change projections for European impact research. Regional Environ. Change 14 (2), 563–578.
Kriegler, E., Edmonds, J., Hallegatte, S., Ebi, K., Kram, T., Riahi, K., Winkler, H., van Vuuren, D., 2014. A new scenario framework for climate change research: the concept of shared policy assumptions. Climatic Change 122, 401–414.
Kropf, C.M., Ciullo, A., Otth, L., Meiler, S., Rana, A., Schmid, E., McCaughey, J.W., Bresch, D.N., 2022. Uncertainty and sensitivity analysis for probabilistic weather and climate risk modelling: an implementation in CLIMADA vol 3.1.0. EarthArXiv, In review.
Lowe, J.A. et al., 2018. UKCP18 science overview report. Technical report.
Lüthi, S., Aznar-Siguan, G., Fairless, C., Bresch, D.N., 2021. Globally consistent assessment of economic impacts of wildfires in CLIMADA v2.2. Geosci. Model Dev. 14, 7175–7187.
Masterton, J., Richardson, F., 1979. Humidex: a method of quantifying human discomfort due to excessive heat and humidity. Environment Canada. Atmos. Environ.
Merkle, M., Alexander, P., Brown, C., Seo, B., Harrison, P.A., Harmackova, Z.V., Pedde, S., Rounsevell, M., 2022. Downscaling population and urban land use for socio-economic scenarios in the UK. Reg. Environ. Change 22 (106).
Met Office (2018). Ukcp18 guidance: Bias correction. Technical report.
Murphy, J., Harris, G., Sexton, D., Kendon, E., Bett, P., Clark, R., Yamazaki, K., 2019. Ukcp18 land projections: Science report. Technical report.
Mylona, A., 2012. The use of UKCP09 to produce weather files for building simulation. Build. Serv. Eng. Res. Technol. 33 (1), 51–62.
New, M., Lopez, A., Dessai, S., Wilby, R., 2007. Challenges in using probabilistic climate change information for impact assessments: an example from the water sector. Philos. Trans. Roy. Soc. A: Math., Phys. Eng. Sci. 365 (1857), 2117–2131.
Nikulin, G., et al., 2018. The effects of 1.5 and 2 degrees of global warming on Africa in the CORDEX ensemble. Environ. Res. Lett. 13 (6), 065003.
O'Neill, B., Kriegler, E., Riahi, K., Ebi, K., Hallegatte, S., Carter, T., Mathur, R., van Vuuren, D., 2015. A new scenario framework for climate change research: the concept of Shared Socioeconomic Pathways. Clim. Change 122, 387–400.
Paulik, R., Horspool, N., Woods, R., Griffiths, N., Beale, T., Magill, C., Wild, A., Popovich, B., Walbran, G., Garlick, R., 2022. RiskScape: a flexible multi-hazard risk modelling engine. Nat. Hazards pages 1573–0840.
Pianosi, F., Beven, K., Freer, J., Hall, J.W., Rougier, J., Stephenson, D.B., Wagener, T., 2016. Sensitivity analysis of environmental models: A systematic review with practical workflow. Environ. Modell. Softw. 79, 214–232.
Pianosi, F., Sarrazin, F., Wagener, T., 2015. A matlab toolbox for global sensitivity analysis. Environ. Model. Software 70, 80–85.
Pianosi, F., Wagener, T., 2015. A simple and efficient method for global sensitivity analysis based on cumulative distribution functions. Environ. Model. Software 67, 1–11.
Pianosi, F., Wagener, T., 2018. Distribution-based sensitivity analysis from a generic input-output sample. Environ. Model. Software 108, 197–207.
Rana, R., Kusy, B., Jurdak, R., Wall, J., Hu, W., 2013. Feasibility analysis of using humidex as an indoor thermal comfort predictor. Energy Build 64, 17–15.
Riahi, et al., 2017. The Shared Socioeconomic Pathways and their energy, land use, and greenhouse gas emissions implications: An overview. One Earth 42, 153–168.
Roy, B., Khan, M.S.M., Islam, A.K.M.S., Khan, M.J.U., Mohammed, K., 2021. Integrated flood risk assessment of the Arial Khan River under changing climate using IPCC AR5 risk framework. J. Water Climate Change 12 (7), 3421–3447.
Saltelli, A., Aleksankin, K., Becker, W., Fennelle, P., Ferretti, F., Holst, N., Li, S., Wu, Q., 2019. Why so many published sensitivity analyses are false: A systematic review of sensitivity analysis practices. Environ. Model. Software 114, 29–39.
Saltelli, A., Annoni, P., Azzini, I., Campolongo, F., Ratto, M., Tarantola, S., 2010. Variance based sensitivity analysis of model output. design and estimator for the total sensitivity index. Comput. Phys. Commun. 181, 259–270.
Sharma, J., Ravindranath, N.H., 2019. Applying IPCC 2014 framework for hazard-specific vulnerability assessment under climate change. Environ. Res. Commun. 1, 051004.
Simpson, et al., 2021. A framework for complex climate change risk assessment. One Earth 4 (4), 489–501.
Sippel, S., Otto, F.E.L., Forkel, M., Allen, M.R., Guillod, B.P., Heimann, M., Reichstein, M., Seneviratne, S.I., Thonicke, K., Mahecha, M.D., 2016. A novel bias correction methodology for climate impact simulations. Earth Syst. Dynam. 7, 71–88.
Smirnov, N.V., 1948. Table for estimating the goodness of fit of empirical distributions. Ann. Math. Statist. 19, 279–281.
Smith, J.Q., 2010. Bayesian Decision Analysis: Principles and Practice. Cambridge University Press, New York.
Stalhandske, Z., Nesa, V., Zumwald, M., Ragettli, M.S., Galimshina, A., Holthausen, N., Röösli, M., Bresch, D.N., 2022. Projected impact of heat on mortality and labour productivity under climate change in Switzerland. Nat. Hazards Earth Syst. Sci. 22, 2531–2541.
Stenning, J., Dellaccio, O., Dicks, J., Harrison, P., Merkle, M., and Rounsevell, M. (2021). Uk-ssps user manual. Technical report.
Strauss, B.H., Orton, P.M., Bittermann, K., Buchanan, M.K., Gilford, D.M., Kopp, R.E., Kulp, S., Massey, C., de Moel, H., Vinogradov, S., 2021. Economic damages from hurricane sandy attributable to sea level rise caused by anthropogenic climate change. Nat. Commun. 12 (2729).
Switanek, M.B., Troch, P.A., Castro, C.L., Leuprecht, A., Chang, H.I., Mukherjee, R., Demaria, E., 2017. Scaled distribution mapping: A bias correction method that preserves raw climate model projected changes. Hydrol. Earth Syst. Sci. 21, 2649–2666.
Thompson, E.L., Smith, L.A., 2019. Escape from model-land. Economics 13 (405).
Thompson, V., Dunstone, N.J., Scaife, A.A., Smith, D.M., Slingo, J.M., Brown, S., Belcher, S.E., 2017. High risk of unprecedented UK rainfall in the current climate. Nat. Commun. 8, 107.
Viner, D., Ekstrom, M., Hulbert, M., Warner, N.K., Wreford, A., Zommers, Z., 2020. Understanding the dynamic nature of risk in climate change assessments: A new starting point for discussion. Atmos. Sci. Lett. 21 (4), e958.
World Health Organisation, 2022. Heatwaves. https://www.who.int/health-topics/heatwaves. Accessed: 2022-05-24.